Many-body electrostatic interactions in electrorheological fluids

Please check the document version of this publication:

• A submitted manuscript is the version of the article upon submission and before peer-review. There can be important differences between the submitted version and the official published version of record. People interested in the research are advised to contact the author for the final version of the publication, or visit the DOI to the publisher's website.
• The final author version and the galley proof are versions of the publication after peer review.
• The final published version features the final layout of the paper including the volume, issue and page numbers.

[Link to publication](#)

Many-body electrostatic interactions in electrorheological fluids

H. J. H. Clercx* and G. Bossis

*Laboratoire de Physique de la Matière Condensée, Université de Nice–Sophia Antipolis,
Parc Valrose, 06108 Nice Cédex 2, France*

We present a general method based on a multipole-expansion theory that allows us to calculate efficiently and accurately the electrostatic forces and the dielectric constant of an assembly of spheres. This method is applied to the study of two aspects which play an important role in the behavior of electrorheological (ER) fluids. The first one concerns the calculation of the principal values $\epsilon_\parallel$ and $\epsilon_\perp$ of the dielectric tensor of the body-centered-tetragonal (bct) lattice, and the calculation of the induced dipole on the particles in this lattice. These are rigorous calculations on physical properties of interest in the study of ER fluids. These results support the idea that the columnlike aggregates which have been found in ER fluids should have a bct structure. Although calculations based on the dipolar approach were previously presented, no results are available that confirm this idea rigorously. The second point concerns an exact analytical derivation of an expression describing the many-body electrostatic forces among spherical polarizable particles in terms of the multipole moments. We have compared this force expression, in the case of two-particle interactions, to some results from the literature. It agrees very well with some analytical two-particle expressions for perfectly conducting spheres and also with some recent results concerning the interactions between two polarizable spheres. Furthermore, we present results for three-particle contributions to the electrostatic force and show that these contributions are unexpectedly large. In particular, the rate of divergence of the force between two conducting spheres can be considerably changed by the presence of a third one.

PACS number(s): 83.80.Gv, 41.20.−q

I. INTRODUCTION

The interest in electrorheological (ER) fluids has grown sharply in recent years. This is related to the possible technical applications of ER fluids and also to the experimental and theoretical developments concerning the study of this class of suspensions. An ER fluid consists of polarizable particles in a nonconducting fluid. It is assumed that the dielectric mismatch between the particle and the fluid is large. If an external electric field is applied to an ER fluid, the particles aggregate and form chains parallel with the applied field. These chains finally aggregate to columnlike structures, completing a phase separation process. In experiments it is possible to see fibrous structures which span the entire distance between the electrodes. This behavior can be understood by considering the dipolar approach; dipoles attract each other if their interparticle axis is parallel to the external field, and repel each other if the interparticle axis is perpendicular to the external field. It should be emphasized that the electrostatic interactions are more complex than described above. For a short review of recent developments in the study of ER fluids we refer to a review paper of Halsey [1].

One of the topics in the study of ER fluids concerns the internal structure of the aggregates which exist in these fluids if an electric field is applied. Recently some results have been reported concerning the internal structure of the columnlike structures arising in ER fluids. Tao and Sun have proposed a body-centered-tetragonal (bct) lattice for the three-dimensional ground state of an ER fluid [2]. They have drawn this conclusion by comparing the electrostatic ground state of several lattice structures with point dipoles on their lattice sites. It is generally assumed that this approach should contain the main physics because only the dipolar interactions are long ranged. Actually, in the case of particles having high polarizabilities with respect to the ambient fluid and for dense structures the multipolar approach should be used to obtain more accurate results. In ER fluids both aspects play an important role. Furthermore it has been shown that the difference of the energy per particle is small if compared to some other lattice structures, such as the face-centered-cubic (fcc) or hexagonal-close-packed (hcp) structures, in the point-dipole approximation roughly 5% (even less than 1% if a multipolar approach is used, as shown in this paper). It should be noted that surface effects might then play a role, and, at finite temperatures, also entropic terms may become important in determining the equilibrium structure. Using a laser-beam diffraction experiment, Chen, Zitter, and Tao have presented evidence for the bct lattice structure inside the columns in an ER fluid of glass spheres [3]. It should be emphasized that the columns may be interpreted as quasi-three-dimensional structures because the columns have a width of order $a(L/a)^{2/3}$, with a the particle radius and L the distance between two parallel electrodes, and $L \gg a$ [4,5]. Also numerical evidence exists using a Monte Carlo simulation [6]. Davis has pointed out that the dipolar approach could only be valid in the case of a small dielectric mismatch, or $\beta = (\alpha-1)/(\alpha+2) \ll 1$, with $\alpha = \epsilon_p/\epsilon_f$ the ratio of particle to fluid dielectric constant [7]. Using a method introduced by Batchelor and O'Brien [8] Davis has shown that for conducting spheres

($\alpha = \infty$) three lattice structures have the same electrostatic ground state, the fcc, the hcp, and the bct structures. He has also considered columns with the lattice structures mentioned above. The existence of a surface leads to a surface energy contribution to the electrostatic energy, and calculations with conducting particles on the lattice sites show that under this circumstance the bct lattice structure is favored. Davis has furthermore assumed that for intermediate dielectric mismatch the three-dimensional bct structure is favorable, even without the stabilizing effects of the presence of a boundary, but no convincing theoretical evidence exists at the moment to support this idea. Some recent results of surface energies of slabs of polarizable particles using a constant dipole approximation [9] and a multipolar approach [10] suggest that the balance which will favor one structure rather than another one might be more subtle.

In this paper we present exact results for the effective dielectric constants of the bct array. Because of the anisotropy of the bct lattice, which is uniaxial, two distinct dielectric constants exist. Furthermore we give exact results for the induced dipole moments on the particles in a bct lattice. These induced dipole moments are necessary to obtain the electrostatic energy per particle, which is needed to decide about the relative stability of the bct lattice in comparison with, e.g., the fcc lattice. For this purpose we have used a general method to study many-particle electrostatic interactions among spherical particles which has been made suitable for calculations of electrostatic properties of periodic arrays. We want to emphasize that the presented method is easily applicable to any kind of lattice. Our method is based on the theory of multipole expansions [11] which has already been used very intensively to study two-particle electrostatic interactions, or many-particle electrostatic interactions with special particle configurations. Some examples are the problem of an infinite chain of spherical particles or regular arrays of particles (see, e.g., Refs. [12–16] for some results where the multipole expansion has been used). However, as far as we know, no results are available for random configurations of particles appropriate to study some aspects of ER fluids. To check the reliability of our method we have compared results for dielectric constants of the three cubic arrays [simple cubic (sc), bcc, fcc] obtained with our method with those of McPhedran and McKenzie [13], and of Sangani and Acrivos [14]. The agreement with their results is excellent.

Besides the presentation of a numerically efficient method to determine the multipole moments we have also succeeded in obtaining an exact expression for the electrostatic force exerted on an arbitrary particle in terms of the so-called generalized multipole moments. This many-body expression has been compared with results of two-particle electrostatic interactions. Also in this case the agreement with data from the literature is perfect. We want to emphasize that with the presented method it is even possible to study the two-particle electrostatic force for high values of α (the ratio of particle to fluid dielectric constant) up to touching spheres. With a method formerly introduced by Klingenberg et al. this was not possible [17]. Even for low values of α, when

multipolar contributions are not too important, an extrapolation technique has been used to obtain the electrostatic force on nearly touching spheres [18]. With the many-body expression we have also studied the electrostatic force exerted on a particle in a three-particle cluster. It seems that the three-particle contribution is of the same order as the two-particle contribution and depends strongly on the cluster geometry. The force expression may be used to study the rupture of solidlike structures encountered in ER fluids, e.g., the way these structures might break. Furthermore it might also be used in simulation techniques to predict the trajectories of the particles in ER suspensions [19].

In Secs. II and III we present the theory which deals with many-particle electrostatic interactions. We have made a distinction between a random-particle approach (Secs. III A and III B) and the case of periodic arrays of polarizable spheres (Sec. III C). In Sec. IV we have presented some values of the effective dielectric constants of cubic lattices and compared them with results from the literature. We also have presented values for the dielectric constants of the bct lattice. The fifth section deals with the stability of the bct lattice in comparison with the fcc lattice. Then, in Sec. VI, we present an exact theoretical derivation of an equation which expresses the electrostatic force on a particle in terms of the multipole moments. In Sec. VII this analytical expression is compared to the numerical results obtained by Klingenberg [20,17] for the two-particle case. The three-particle contribution to the electrostatic force has been studied for two special configurations. The results are presented in Sec. VIII. A short conclusion will end this paper.

II. THE GRAND POTENTIAL MATRIX

We consider a system of N spherical particles immersed in an unbounded fluid. The particles have a dielectric constant ϵ_p, and the fluid has a dielectric constant ϵ_f. We do not make any restrictions concerning the values of ϵ_p and ϵ_f, but it is obvious that the case $\epsilon_p = \epsilon_f$ is of no interest to us. All particles have the same radius a and they have position vectors $\mathbf{R}_i$, $i \in \{1, \ldots, N\}$, with respect to an arbitrary chosen origin. This system is acted upon by a constant external electric field $\mathbf{E}_0$. For our purpose in this section it is more convenient to study the potential problem. The external potential is then

$$\varphi_0(\mathbf{r}) = -\mathbf{E}_0 \cdot \mathbf{r} \ . \tag{2.1}$$

No free charges are present in the system. Consequently, to obtain the potential in the system, we have to solve the Laplace equation:

$$\Delta \varphi(\mathbf{r}) = 0 \ , \tag{2.2}$$

using the following boundary conditions at the surfaces of all the particles in the fluid:

$$\varphi_{\text{in}}^i(\mathbf{r}_i) = \varphi_{\text{out}}(\mathbf{r}_i), \quad \text{with } \mathbf{r}_i \in S_i \ , \tag{2.3}$$

$$\alpha \frac{\partial \varphi_{\text{in}}^i(\mathbf{r}_i)}{\partial r_i} = \frac{\partial \varphi_{\text{out}}(\mathbf{r}_i)}{\partial r_i}, \quad \text{with } \mathbf{r}_i \in S_i \ , \tag{2.4}$$

$\varphi_{\text{in}}^i(\mathbf{r}_i)$ is the potential inside particle i, with $i \in \{1, \ldots, N\}$, and $\varphi_{\text{out}}(\mathbf{r}_i)$ is the potential inside the fluid. The potentials are defined with respect to the center of particle i, with $\mathbf{r} = \mathbf{r}_i + \mathbf{R}_i$. S_i is the surface of particle i and finally $\alpha = \epsilon_p / \epsilon_f$, the ratio between the particle and the fluid dielectric constants. We have used the spherical symmetry of the particles in Eq. (2.4). It is known from many textbooks on boundary-value problems in electrostatics that a unique solution of the Laplace equation (2.2) exists which satisfies the boundary conditions (2.3) and (2.4), e.g., Ref. [11]. We have studied this problem using the theory of multipole expansions. Knowing the potential, the electric field $\mathbf{E}(\mathbf{r})$ is known as a function of $\mathbf{r}$ via the relation $\mathbf{E}(\mathbf{r}) = -\nabla\varphi(\mathbf{r})$ and the electric displacement is given by $\mathbf{D}(\mathbf{r}) = \epsilon\mathbf{E}(\mathbf{r})$, assuming an isotropic medium, which is correct within the particles and inside the fluid.

In this paper we shall express the potential inside the fluid in terms of multipole moments. The externally imposed electric field and the multipole moments are related through a linear relation:

$$\phi = \underline{Z} \cdot \mathbf{Q} \ . \tag{2.5}$$

The vector ϕ represents all derivatives of the external potential at the origin of all N particles [i.e., $\nabla_i^n \varphi_{\text{out}}(\mathbf{r}_i = \mathbf{0})$, with $n = 0, 1, 2$, etc. and $i \in \{1, \ldots, N\}$]. The vector $\mathbf{Q}$ represents all components of the multipole moments belonging to the N particles. The matrix $\underline{Z}$ is composed of N^2 tensors:

$$\underline{Z} = \begin{bmatrix} \underline{Z}_{11} & \cdots & \underline{Z}_{1N} \\ \vdots & & \vdots \\ \underline{Z}_{N1} & \cdots & \underline{Z}_{NN} \end{bmatrix} \ , \tag{2.6}$$

and each tensor $\underline{Z}_{ij}$, which relates the multipole moments of particle j with the derivatives of the externally applied potential at the center of particle i, depends on the geometry of the N-particle cluster only, and can be determined for a special configuration without reference to the applied potential field. Reciprocally there are no induced multipole moments on the particles if the external field is zero.

A special version of the matrix $\underline{Z}$ is used in the study of the induced dipoles on charge-free polarizable particles, which we call the grand potential matrix $\underline{\Pi}$ (Bonnecaze and Brady [21]):

$$\mathbf{E} = \underline{\Pi} \cdot \mathbf{M} \ , \tag{2.7}$$

with $\mathbf{E}$ a $3N$-column vector whose components are the externally applied electric field at the center of the N particle and $\mathbf{M}$ also a $3N$-column vector with the induced dipole moments on the N particles. Of course, the grand potential matrix depends also on the geometric configuration of the particles only. The grand potential matrix is the analog of the grand mobility matrix in low Reynolds number fluid dynamics.

Finally we introduce an expression for the force exerted by the particles (and the external field) on a reference particle. The force on this spherical particle can be found by integration of the Maxwell stress tensor over the surface of the sphere. The Maxwell stress tensor is defined by (assuming the absence of magnetic fields) [11]

$$\underline{T}(\mathbf{r}) = \frac{1}{4\pi} \left[\mathbf{E}(\mathbf{r})\mathbf{D}(\mathbf{r}) - \frac{1}{2}\underline{I}[\mathbf{E}(\mathbf{r}) \cdot \mathbf{D}(\mathbf{r})] \right] \ . \tag{2.8}$$

Consequently, we have for the force on the reference particle

$$\mathbf{F} = a^2 \int_{|r| = a} \underline{T}(\mathbf{r}) \cdot \hat{\mathbf{e}}_r d\Omega \ , \tag{2.9}$$

with $\hat{\mathbf{e}}_r$ the radial unit vector in a spherical coordinate system and $d\Omega$ the element of solid angle. In Sec. VI we show that it is possible to derive an analytical expression for $\mathbf{F}$ in terms of multipole moments.

III. GENERAL SOLUTION OF THE LAPLACE EQUATION

A. The general set of linear equations

It is generally known how to solve the Laplace equation (2.2) for this kind of problem [11,13]. For this reason we only give here a short outline of the derivation.

The external potential, as introduced in Sec. II, is defined with respect to an arbitrary origin. However, to use the boundary conditions (2.3) and (2.4) it is necessary to define the external potential with respect to the respective particle centers. Relatively to the origin of particle i (with $\mathbf{r} = \mathbf{r}_i + \mathbf{R}_i$), we have

$$\varphi_0(\mathbf{r}_i + \mathbf{R}_i) = -\mathbf{E}_0 \cdot \mathbf{r}_i - \mathbf{E}_0 \cdot \mathbf{R}_i = \varphi_0(\mathbf{r}_i) + \psi_i \ . \tag{3.1}$$

The difference of the particle dielectric constant and that of the fluid ($\alpha \neq 1$) results, in addition to the external potential, in a contribution to the potential fields inside and outside the particles. The potential inside and outside particle i may be expanded in terms of solid spherical harmonics, a method among others used by McPhedran and McKenzie [13] to study the conductivity of arrays of conducting spherical particles. The potential inside particle i is, using spherical symmetry,

$$\varphi_{\text{in}}^i(\mathbf{r}_i) = \psi_i + \varphi_0(\mathbf{r}_i) + \sum_{\substack{l\,(\geq 0) \\ m}} \beta_{lm}^i r_i^l Y_{lm}(\theta_i, \varphi_i) \ , \tag{3.2}$$

with $Y_{lm}(\theta_i, \varphi_i)$ spherical harmonics defined with respect to the center of particle i and β_{lm}^i the expansion coefficients. We need those solid spherical harmonics which behave regularly for $|r| \to 0$. Equation (3.2) is, of course, valid for each $i \in \{1, \ldots, N\}$. The potential in the fluid surrounding particle i is a sum of contributions from all the particles in the system (and the external potential). Of course, these contributions consist of solid spherical harmonics which behave regularly for $|\mathbf{r}| \to \infty$. The potential inside the fluid has the form

$$\varphi_{\text{out}}(\mathbf{r}_i) = \psi_i + \varphi_0(\mathbf{r}_i)$$
$$+ \sum_{\substack{l\,(\geq 0) \\ m}} \frac{4\pi}{2l+1} Q_{lm}^i r_i^{-(l+1)} Y_{lm}(\theta_i, \varphi_i)$$
$$+ \sum_{j\,(\neq i)} \sum_{\substack{l\,(\geq 0) \\ m}} \frac{4\pi}{2l+1} Q_{lm}^j r_j^{-(l+1)} Y_{lm}(\theta_j, \varphi_j) \ , \tag{3.3}$$

where the last term expresses the field due to the other particles. The multipole moments Q_{lm}^i are defined in the following way [11]:

$$Q_{lm}^i = \int_{V_i} Y_{lm}^*(\theta,\varphi) r^l \rho(\mathbf{r}) dV \ , \tag{3.4}$$

with V_i the volume of particle i and $\rho(\mathbf{r})$ the charge density inside particle i. For each particle we can formulate such an equation and a set of linear equation of the coefficients $\{Q_{lm}^i, \beta_{lm}^i\}$, $i \in \{1, \ldots, N\}$, can be obtained by using the boundary conditions [Eqs. (2.3) and (2.4)] and the orthonormality relations of the spherical harmonics. Furthermore it can be shown that it is possible

to express all the coefficients β_{lm}^i in terms of the multipole moments Q_{lm}^i. However, before we can use the orthonormality relations for the $Y_{lm}(\theta_i,\varphi_i)$, with the center of particle i as origin, it is necessary to express the solid spherical harmonics, defined with respect to the center of particle j, in terms of solid spherical harmonics defined with respect to the center of particle i. The formulas needed for this reformulation are the so-called Hobson formulas. We use for this purpose the same notation as used in earlier papers by one of the authors concerning a study of N-particle hydrodynamic interactions in suspensions [22,23]. For more details and references, see these two papers. Equation (3.3) can be rewritten as follows:

$$\varphi_{\text{out}}(\mathbf{r}_i) = \psi_i + \varphi_0(\mathbf{r}_i) + \sum_{\substack{l \, (\geq 0) \\ m}} \frac{4\pi}{2l+1} Q_{lm}^i r_i^{-(l+1)} Y_{lm}(\theta_i,\varphi_i)$$

$$+ \sum_{\substack{s \, (\geq 0) \\ t}} \frac{n_{st}}{(s+t)!} r_i^s Y_{st}(\theta_i,\varphi_i) \sum_{j \, (\neq i)} \left[\sum_{\substack{l \, (\geq 0) \\ m}} \frac{4\pi}{2l+1} Q_{lm}^j M_{lm;st}^{ji}(\mathbf{R}_{ij}) \right] \ . \tag{3.5}$$

In this expression we have used the following shorthand notations:

$$n_{st} = \left[\frac{4\pi}{(2s+1)} \frac{(s+t)!}{(s-t)!} \right]^{1/2} \tag{3.6}$$

and

$$M_{lm;st}^{ji} = (-1)^{s+t} \frac{(l+s-m+t)!}{n_{lm}(l-m)!} n_{l+s,m-t} \frac{Y_{l+s,m-t}(\xi_{ij}\eta_{ij})}{R_{ij}^{l+s+1}} \ , \tag{3.7}$$

with ξ_{ij} and η_{ij} the polar and azimuthal angles of the vector $\mathbf{R}_{ij} = \mathbf{R}_i - \mathbf{R}_j$. This expression is obtained from the general form of the Hobson formula.

By substituting Eqs. (3.2) and (3.5) into the equation of boundary condition (2.3) for $\varphi_{\text{in}}^i(\mathbf{r}_i)$ and $\varphi_{\text{out}}(\mathbf{r}_i)$, respectively, and applying the orthonormality condition of the spherical harmonics, we obtain the following result:

$$\beta_{pq}^i = \frac{4\pi}{2p+1} a^{-(2p+1)} Q_{pq}^i + \frac{n_{pq}}{(p+q)!} \sum_{j \, (\neq i)} \left[\sum_{\substack{l \, (\geq 0) \\ m}} \frac{4\pi}{2l+1} Q_{lm}^j M_{lm;pq}^{ji}(\mathbf{R}_{ij}) \right] \ . \tag{3.8}$$

Substituting the normal derivatives of Eqs. (3.2) and (3.5) into the equation of boundary condition (2.4) for $\partial \varphi_{\text{in}}^i(\mathbf{r}_i)/\partial r_i$ and $\partial \varphi_{\text{out}}(\mathbf{r}_i)/\partial r_i$, respectively, and applying also the orthonormality condition of the spherical harmonics gives the second set of equations:

$$(1-\alpha)\delta_{p,1} \left[n_{10} E_{0z} \delta_{q,0} - \frac{1}{2} n_{11}(E_{0x} - iE_{0y})\delta_{q,1} + \frac{1}{2} n_{11}(E_{0x} + iE_{0y})\delta_{q,-1} \right] + \alpha p a^{p-1} \beta_{pq}^i$$

$$= -4\pi \frac{p+1}{2p+1} a^{-(p+2)} Q_{pq}^i + p a^{p-1} \frac{n_{pq}}{(p+q)!} \sum_{j \, (\neq i)} \left[\sum_{\substack{l \, (\geq 0) \\ m}} \frac{4\pi}{2l+1} Q_{lm}^j M_{lm;pq}^{ji}(\mathbf{R}_{ij}) \right] \ . \tag{3.9}$$

The quantities E_{0x}, E_{0y}, and E_{0z} are the components of the externally applied electric field and i is the imaginary unit. The constants n_{10} and n_{11} are special cases of the n_{st} defined in Eq. (3.6). Substituting Eq. (3.8) into Eq. (3.9) for β_{pq}^i gives the result

$$\beta_1 a^3 \delta_{p,1} \left[n_{10} E_{0z} \delta_{q,0} - \frac{1}{2} n_{11}(E_{0x} - iE_{0y})\delta_{q,1} + \frac{1}{2} n_{11}(E_{0x} + iE_{0y})\delta_{q,-1} \right]$$

$$= \frac{4\pi}{2p+1} Q_{pq}^i + \beta_p a^{2p+1} \frac{n_{pq}}{(p+q)!} \sum_{j \, (\neq i)} \left[\sum_{\substack{l \, (\geq 0) \\ m}} \frac{4\pi}{2l+1} Q_{lm}^j M_{lm;pq}^{ji}(\mathbf{R}_{ij}) \right] \ , \tag{3.10}$$

with β_p (and β_1) a shorthand notation for

$$\beta_p = \frac{p(\alpha-1)}{\{p(\alpha+1)+1\}} . \tag{3.11}$$

This infinite set of linear algebraic equations for the multipole moments $\{Q_{lm}^1, \ldots, Q_{lm}^N\}$ is sufficient to determine the matrix $\underline{Z}$ [Eq. (2.5)] or the grand potential matrix $\underline{\Pi}$. It is not very difficult to present Eq. (3.10) in matricial notation:

$$\begin{bmatrix} \mathbf{E}_1 \\ \vdots \\ \mathbf{E}_N \end{bmatrix} = \begin{bmatrix} \underline{Z}_{11} & \cdots & \underline{Z}_{1N} \\ \vdots & & \vdots \\ \underline{Z}_{N1} & \cdots & \underline{Z}_{NN} \end{bmatrix} \cdot \begin{bmatrix} \mathbf{Q}_1 \\ \vdots \\ \mathbf{Q}_N \end{bmatrix} , \tag{3.12}$$

with all $\mathbf{E}_i = (0, \mathbf{E}, 0, \ldots,)$ and $\mathbf{Q}_i = \{Q_{lm}^i; l \geq 0, |m| \leq l\}$. The matrix components of $\underline{Z}_{ij}$ can be derived from Eq. (3.10). To determine the grand potential matrix it is necessary to solve the set of linear equations (3.10) in such a way that we express all multipole moments $\{Q_{lm}^1, \ldots, Q_{lm}^N\}$, with $l \geq 2$ and $|m| \leq l$, in terms of the multipole moments $\{Q_{1,m}^1, \ldots, Q_{1,m}^N\}$, with $|m| \leq 1$. These moments are related with the induced dipole moments on the N particles via [11]

$$n_{10}Q_{1,0}^i = M_{i,z}, \quad n_{11}Q_{1,1}^i = -M_{i,x} + iM_{i,y} , \tag{3.13}$$

$$n_{11}Q_{1,-1}^i = M_{i,x} + iM_{i,y} .$$

This operation is in fact a partial inversion of the matrix defined in Eq. (3.12).

An important aspect of the set of linear equations is worthwhile to be emphasized. The multipole moments $\{Q_{0,0}^1, \ldots, Q_{0,0}^N\}$ appear naturally in the set of linear equations, but writing down explicitly the equations with $p = 0$ and $q = 0$ leads to the conclusion that these moments are all zero. The reason is the absence of free charges on the particles.

The set of linear equations derived in this section has an infinite number of unknowns. It is possible to solve this set of linear equations if we define an upper limit for the allowed values of l and p, e.g., $l_{max} = p_{max} = L$. This restriction is in fact the assumption that the set of multipole moments $\{Q_{lm}^1, \ldots, Q_{lm}^N\}$ is zero for all $l > L$.

With the upper limit L we obtain $L(L+2)N$ linear equations with the same number of unknown multipole moments. We call the solution the so-called Lth order solution of the set of linear equations. The choice of the upper limit L depends on several factors, the most important being the desired numerical accuracy with which the multipole moments should be calculated and the convergence behavior with increasing L of the multipole moments in which we are interested.

B. Reformulation of the set of linear equations for numerical calculations

The set of equations derived in the preceding section is not suitable for efficient numerical calculations. A reformulation like the one used in [23] facilitates the calculations considerably. This reformulated set of equations has been used in the study of the three-particle contributions to the electrostatic force which are presented in this paper. Furthermore an adapted version has been used in the following section in the case of periodic arrays.

Let us define the generalized multipole moments $A_{lm}^{\pm i}$ via the following transformations:

$$[Q_{lm}^i \pm (-1)^m Q_{l,-m}^i] = \frac{2l+1}{4\pi} n_{lm} a^{l+2} (-1)^{l+m} A_{lm}^{\pm i} , \tag{3.14}$$

$$A_{l,-m}^{\pm i} = \pm(-1)^m \frac{(l+m)!}{(l-m)!} A_{lm}^{\pm i} .$$

We see from the relations for the generalized multipole moments $A_{lm}^{\pm i}$ that it is sufficient to use the plus coefficients, A_{lm}^{+i} etc., with $m \geq 0$, and the minus ones, A_{lm}^{-i} etc., with $m > 0$, in the set of independent coefficients. We introduce these generalized multipole moments to simplify the set of linear equations mathematically. There is also a physical interpretation because the moments $A_{lm}^{\pm i}$ are proportional to the potential field and its derivatives evaluated at $\mathbf{R}_i$ due to the external potential and the presence of the other spheres. See in this context the discussion about electrostatic Faxén laws by Bonnecaze and Brady [21]. We do not present the total derivation of the rewritten set of linear equations but the final result only, which comes to

$$-\beta_1 \delta_{p,1}(2E_{0z}\delta_{q,0} + E_{0x}\delta_{q,1}) = A_{pq}^{+i} + \beta_p \sum_{\substack{j\,(\neq i) \\ m\,(\geq 0)}} \sum_{l\,(\geq 1)} \mathrm{Re}[P_{lm;pq}^{+ji}]x_{ij}^{l+p+1}A_{lm}^{+j} + i\beta_p \sum_{\substack{j\,(\neq i) \\ m\,(\geq 1)}} \sum_{l(\geq 1)} \mathrm{Im}[P_{lm;pq}^{-ji}]x_{ij}^{l+p+1}A_{lm}^{-j} , \tag{3.15}$$

$$i\beta_1 \delta_{p,1}E_{0y}\delta_{q,1} = A_{pq}^{-i} + \beta_p \sum_{\substack{j\,(\neq i) \\ m\,(\geq 1)}} \sum_{l\,(\geq 1)} \mathrm{Re}[P_{lm;pq}^{-ji}]x_{ij}^{l+p+1}A_{lm}^{-j} + i\beta_p \sum_{\substack{j(\neq i) \\ m\,(\geq 0)}} \sum_{l\,(\geq 1)} \mathrm{Im}[P_{lm;pq}^{+ji}]x_{ij}^{l+p+1}A_{lm}^{+j} , \tag{3.16}$$

with $x_{ij} = a/R_{ij}$. In these equations we have introduced the following shorthand notations:

$$P_{lm;pq}^{\pm ji} = \left[1 - \frac{1}{2}\delta_{m,0}\right]\frac{(-1)^{l+p+m+q}}{(p+q)!}n_{lm}R_{ij}^{l+p+1}$$

$$\times[M_{lm;pq}^{ji}(\mathbf{R}_{ij}) \pm (-1)^m M_{l,-m;pq}^{ji}(\mathbf{R}_{ij})] . \tag{3.17}$$

It is noteworthy to emphasize that the special functions $P_{lm;pq}^{\pm ji}$ are functions of the polar angle ξ_{ij} and azimuthal angle η_{ij} only.

In principle it is possible to solve partially the set of linear algebraic equations if we express all generalized multipole moments $A_{lm}^{\pm i}$, with $l \geq 2$, $|m| \leq l$, and $i \in \{1, \ldots, N\}$, in terms of the generalized multipole mo-

ments $\{A_{10}^{+i}, A_{11}^{+i}, A_{11}^{-i}\}$ with $i \in \{1, \ldots, N\}$. These remaining moments are related to the components of the induced dipole moments on particle i via the following relations:

$$A_{10}^{+i} = -\frac{2}{a^3} M_{i,z}, \quad A_{11}^{+i} = -\frac{1}{a^3} M_{i,x}, \quad A_{11}^{-i} = \frac{i}{a^3} M_{i,y},$$

(3.18)

where we have used Eqs. (3.13) and (3.14). We are now able to calculate (numerically) the components of the grand potential matrix.

C. The set of linear equations suitable for periodic arrays

In this paper we consider two types of lattices. These are the cubic lattices, with the crystal axes coinciding with a Cartesian coordinate system, and the body-centered-tetragonal lattice, with the crystal axis which coincides with the fourfold axis of symmetry parallel with the z axis. On the lattice sites we have put spherical polarizable particles of radius a. We may choose an arbitrary lattice site as the origin of a coordinate system. The positions of the other lattice sites are then denoted by the vector $\mathbf{R}_j$ (with spherical coordinates R_j, ξ_j, and η_j). We assume the presence of an averaged macroscopic electric field $\mathbf{E}$ parallel to the z axis, which is the optical axis of the bct lattice, or the x axis. The latter axis is assumed to be parallel to the twofold symmetry axis of the bct array. For the cubic arrays there is no distinction between both situations in contrast to the bct array. The configuration with the macroscopic field parallel with the optical axis is of special interest in studying the ground state of ER fluids. For the cubic or tetragonal lattices it is possible to simplify the set of linear algebraic equations, presented in Sec. III B, considerably. We do not present details of this reformulation, but some remarks are useful. We have implicitly assumed one particle per unit cell so that each particle is translationally invariant. Consequently all generalized multipole moments with the same indices l and m are equal, $A_{lm}^{\pm j} = A_{lm}^{\pm}$. Furthermore it can be shown that the imaginary parts in the set of linear equations are zero (see discussion below concerning the lattice sums). The final result is a set of linear equations which relates the averaged macroscopic electric field with so-called generalized multipole moments A_{lm}^{+}:

$$-\beta_1 \delta_{p,1} (2E_z \delta_{q,0} + E_x \delta_{q,1})$$
$$= A_{pq}^{+} + \beta_p \sum_{\substack{l \ (\geq 1) \\ m \ (\geq 0)}} X_{lm;pq}^{R+} A_{lm}^{+}.$$

(3.19)

We have introduced the following shorthand notation:

$$X_{lm;pq}^{R+} = \sum_{j \ (\neq 0)} \text{Re}[P_{lm;pq}^{+j}] x_j^{l+p+1},$$

(3.20)

with $x_j = a/R_j$, and $P_{lm;pq}^{+j}$ is defined in Sec. III B. These sums are modified three-dimensional lattice sums which can be determined using a method introduced by Nijboer and de Wette [24]. Using symmetry arguments it is possible to show that we may study separately the two cases

where the averaged macroscopic electric field is parallel to and perpendicular to the xy plane, respectively. Thus Eq. (3.19) can be separated into two independent sets of linear equations, one related with the z component of the macroscopic field and the other with the x component. This set of linear equations can be solved as explained in Sec. III B.

The modified lattice sums in Eq. (3.20) consist of the following elementary lattice sums:

$$S_{lm} = n_{lm} \sum_{j \ (\neq 0)} \frac{Y_{lm}(\xi_j, \eta_j)}{\mathcal{R}_j^{l+1}},$$

(3.21)

with $\mathcal{R}_j = R_j/R$, the lattice vectors nondimensionalized by the particle separation along the x axis. The z axis of the coordinate system coincides with the fourfold axis of symmetry of the lattices under consideration. Consequently we may conclude that $S_{lm} = 0$ is m is not quadruple. This is the mathematical reason of the decoupling of the set of linear equations into equations related with the averaged macroscopic field in the z and x directions, respectively, which is discussed above [see Eq. (3.19)]. Furthermore it can be shown that S_{lm} is always real because the lattice sums always include the pair of lattice points (R_j, ξ_j, η_j) and $(R_j, \xi_j, -\eta_j)$, thus

$$\sum_{j \ (\neq 0)} \text{Im}[P_{lm;pq}^{+j}] x_j^{l+p+1} \equiv 0.$$

(3.22)

The remaining lattice sums can be calculated without difficulty for $l \geq 3$ using an Ewald summation technique. For $l = 2$ the above lattice sum is conditionally convergent. It is sufficiently known how to handle this kind of lattice sums for cubic arrays (see, e.g., McPhedran and McKenzie where this problem has been discussed in more detail [13]). In the same way one is able to obtain the appropriate value for the conditionally convergent lattice sum related with the internal structure of the bct lattice. In this context it is useful to emphasize that the conditionally convergent lattice sums can be obtained by taking the appropriate limits in the reformulated lattice sums introduced by Nijboer and de Wette [24]. In Table I we present the values of the lattice sums obtained for the bct array for $l \leq 8$. Our value of the conditional convergent lattice sum is in agreement with the one used by Tao and Sun in their point-dipole calculations [2]. To obtain accurate results for ϵ_{eff} in the case of (nearly) close packed structures the S_{lm}, with l up to 150, have been used.

TABLE I. The lattice sums for the bct structure for $l \leq 8$.

l,m	S_{lm}^{bct}
2,0($\parallel$)	$+5.603\,391$
2,0($\perp$)	$-9.787\,207$
4,0	$+9.809\,174 \times 10^{-2}$
4,4	$-8.768\,701 \times 10^{2}$
6,0	$+1.758\,071 \times 10^{1}$
6,4	$-1.659\,548 \times 10^{4}$
8,0	$+9.983\,326$
8,4	$+5.704\,327 \times 10^{4}$
8,8	$+4.031\,592 \times 10^{7}$

IV. THE DIELECTRIC CONSTANTS
OF INFINITE PERIODIC ARRAYS

In this section we present results concerning the dielectric constants of the bct lattice. However, we start with some results of a comparison of data of the dielectric constants of several cubic lattices with spherical polarizable particles on the lattice sites. For this comparison we have used some results from the literature obtained by McPhedran and McKenzie [13] and Sangani and Acrivos [14]. We restrict ourselves to the presentation of some dielectric constants of close packed simple cubic, body-centered-cubic, and face-centered-cubic lattices for relative low values of $\alpha = \epsilon_p / \epsilon_f$ (an exception is made for the sc lattice where also some values for $\alpha = \infty$ are considered). The aim of this comparison is to show that our theoretical method is good and its numerical implementation has been carried out correctly.

As expounded in Sec. III the multipole expansion theory has been used to determine accurate values for the induced dipole moment $\mathbf{M}$ and the components of the dielectric tensor $\underline{\epsilon}_{\text{eff}}$ for several periodic arrays. The latter is, of course, diagonal due to our choice of the coordinate system. For the cubic lattices the principal values of the dielectric tensor are equal, but for the bct lattice we can distinguish two different principal values. The principal value related with the optical axis will be denoted by $\epsilon_{\parallel}$, the other values by $\epsilon_{\perp}$. After partial inversion of Eq. (3.19) and using Eq. (3.18), we obtain the following relation between the averaged macroscopic electric field and the induced dipole moment (where we have implicitly used the fact that the y component of the induced dipole moment is equivalent to the x component):

$$\beta_1 a^3 \mathbf{E} = \underline{C} \cdot \mathbf{M} , \qquad (4.1)$$

with $\underline{C}$ a diagonal tensor of proportionality. A simple relation exists for the effective dielectric tensor of the regular array [25,14]:

$$\underline{\epsilon}_{\text{eff}} = \epsilon_f (\underline{I} + 3\beta_1 \varphi \underline{C}^{-1}) . \qquad (4.2)$$

The tensor $\underline{C}$ is trivial for the cubic lattices ($\underline{C} = C\underline{I}$), but for the bct lattice we have, of course, two different values, $C_{\parallel}$ and $C_{\perp}$. It is obvious that $\underline{C}$ is a complicated function of volume fraction and depends strongly on the lattice sums for the respective lattices.

We have made a comparison with some of the available data in the literature. We had to be careful in selecting those data with which we wanted to make the comparison. The data presented by McPhedran and McKenzie for the sc array are obtained with a method which neglects the azimuthal terms [13]. However, their data do not differ very much from ours up to close packed volume fractions. For a more precise comparison we have used some of their exact data for conducting spheres which they presented in the same paper with the intention to show that their approximation was reasonable. For $\varphi = 0.5$ they obtained $\epsilon_{\text{eff}}/\epsilon_f = 5.891$ where we have obtained 5.891 31. For $\varphi = 0.46$ they obtained 4.315 and we calculated 4.314 76. Our data are converged values up to at least the last figure. McKenzie, McPhedran, and

Derrick realized that their assumption concerning the importance of the azimuthal terms did not work very well for the bcc and fcc lattices [26]. However, they have presented results of full calculations and all their data agree perfectly with ours for both the bcc and fcc lattices. Sangani and Acrivos have presented formulas to obtain the effective dielectric constants of the three cubic lattices [14]. Unfortunately they did not present data for the effective dielectric constant for the full range of volume fractions. Bonnecaze and Brady have used the method of Sangani and Acrivos to obtain data for the dielectric constant ϵ_{eff} for three values of α ($\infty, 10, 0.01$) to compare their simulation data with [21]. We have calculated the values of ϵ_{eff} for $\alpha = \infty$ and may conclude that they agree with those of Sangani and Acrivos for the sc and bcc array (within a few parts per thousand for nearly close packed arrays). However, we have found serious differences between our results and those based on the method of Sangani and Acrivos which have been presented by Bonnecaze and Brady for the fcc lattice if $\varphi > 0.6$. The reason seems to be some accuracy problems in their interpolation method for the effective dielectric constant of the fcc lattice (not for the sc or bcc lattice) which has relatively large consequences at high volume fractions. Thus we cannot compare our results with these tabulated data. Considering this discrepancy we want to emphasize that our results are in excellent agreement with those of McKenzie, McPhedran, and Derrick [26], and also with calculations performed by Doyle [27], for $\varphi \le 0.73$. In spite of the discrepancy noted above the method of Sangani and Acrivos is correct. This might be concluded by the fact that they presented exact results for the effective dielectric constant for close packed arrays of particles with low and intermediate relative polarizabilities. These data are convenient and we have tabulated their data together with ours in Table II. The agreement is excellent. On the basis of this comparison and with data presented by McPhedran and McKenzie, McKenzie, McPhedran, and Derrick, and Doyle we may conclude that our method of formulating the infinite set of linear equations leads to good results. This observation is important for the remaining part of the paper, but also for future work on sheared lattice structures. In the latter case we have to apply our method to the most general case of triclinic lattice structures.

TABLE II. The dielectric constants of close packed configurations of the three cubic lattices calculated with our method, denoted by ϵ_{sc}, etc., compared with some available results of Sangani and Acrivos, which are denoted by $\epsilon_{\text{sc}}^{\text{SA}}$, etc. [14]. As far as we know no results are available in the literature for $\alpha = 100$.

α	ϵ_{sc}	$\epsilon_{\text{sc}}^{\text{SA}}$	ϵ_{bcc}	$\epsilon_{\text{bcc}}^{\text{SA}}$	ϵ_{fcc}	$\epsilon_{\text{fcc}}^{\text{SA}}$
0	0.3437	0.344	0.2172	0.217	0.1600	0.160
2	1.4585	1.46	1.6196	1.60	1.6876	1.69
5	2.4224	2.42	3.0352	3.04	3.3588	3.36
10	3.4738	3.47	4.6879	4.69	5.4688	5.47
20	4.814	4.81	6.893	6.89	8.500	8.49
50	6.98	6.9	10.58	10.5	13.97	13.8
100	8.8		13.7		18.9	

TABLE III. The principal values of the dielectric tensor for conducting spherical particles on the lattice sites of the bct array. The results are accurate up to the last figure quoted.

φ	$\epsilon_{\parallel}$	$\epsilon_{\perp}$
0.05	1.159	1.155
0.10	1.337	1.332
0.15	1.538	1.525
0.20	1.768	1.745
0.25	2.033	1.988
0.30	2.341	2.270
0.35	2.707	2.597
0.40	3.149	2.985
0.45	3.699	3.459
0.50	4.411	4.059
0.55	5.385	4.865
0.60	6.853	6.048
0.65	9.576	8.183
0.66	10.50	8.895
0.67	11.73	9.836
0.68	13.52	11.20
0.69	16.84	13.71

FIG. 2. The relative dielectric constants $\epsilon_{\parallel}$ (solid line) and $\epsilon_{\perp}$ (dashed line) as a function of the volume fraction φ for $\alpha = \epsilon_p / \epsilon_f = 10$.

We present now some data concerning the two dielectric constants of the bct lattice. This lattice resembles a compressed bcc lattice and has the lattice vectors $\mathbf{a}_1 = \hat{\mathbf{e}}_x$, $\mathbf{a}_2 = \hat{\mathbf{e}}_y$, and $\mathbf{a}_3 = \frac{1}{3}\sqrt{6}\hat{\mathbf{e}}_z$ (these are not the lattice vectors of the unit cell). The particles are on the lattice sites $k\mathbf{a}_1 + l\mathbf{a}_2 + m\mathbf{a}_3$ and $(k+\frac{1}{2})\mathbf{a}_1 + (l+\frac{1}{2})\mathbf{a}_2 + (m+\frac{1}{2})\mathbf{a}_3$, with $\{k,l,m\} \in Z_3$. The particles on both sets of lattice sites are, of course, translationally invariant. The interest in the physical properties of the bct array has grown since it is a serious candidate for the internal structure of the columnlike aggregates arising in electrorheological fluids. We have calculated $\epsilon_{\parallel}$ and $\epsilon_{\perp}$ for conducting spheres on the lattice sites and presented them in Table III. In Figs. 1–3 we show the dielectric constants as function of φ for $\alpha \in \{0, 10, 100\}$. We have not tabulated or plotted more results; the computer programs to calcu-

late the necessary lattice sums and the components of the dielectric tensor are available upon request from the authors.

Finally we present in Table IV some accurate results for close packed values of $\epsilon_{\parallel}$ and $\epsilon_{\perp}$ for a bct array. The values for $\epsilon_{\parallel}$ especially could be of interest in the study of the dielectric constant of ER fluids. As we approach the limit of conducting spheres it becomes more difficult to obtain accurate values for the dielectric constants, but our data give a good indication of these values. Considering the results from Tables II and IV more closely we see that the dielectric constant of the close packed fcc lattice is larger than the dielectric constant $\epsilon_{\parallel}$ of the close packed bct lattice. If we consider the dipolar approach we see the reverse effect if $\alpha > 25$. This point indicates that one should be cautious in drawing conclusions from a dipolar approach only.
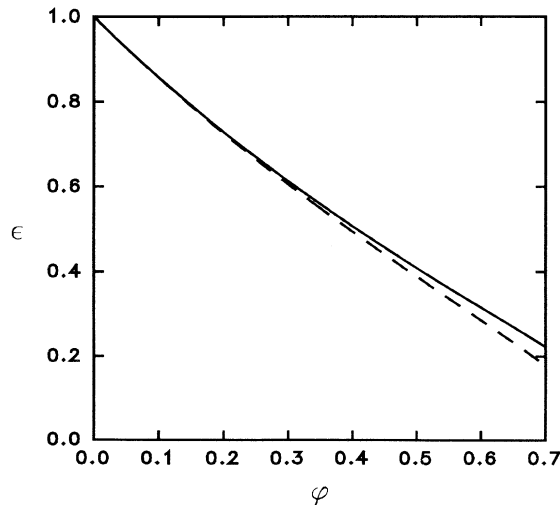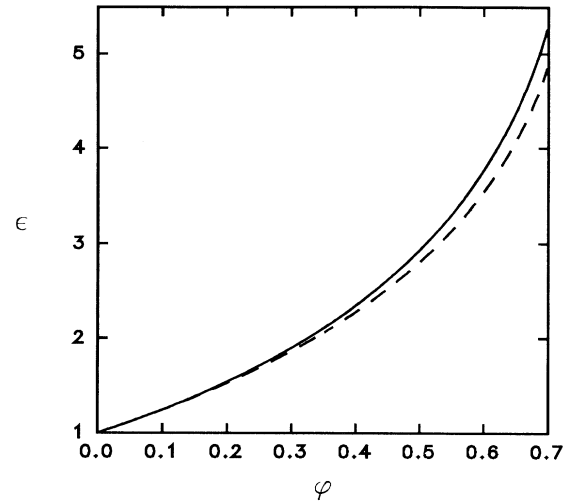

FIG. 1. The relative dielectric constants $\epsilon_{\parallel}$ (solid line) and $\epsilon_{\perp}$ (dashed line) as a function of the volume fraction φ for $\alpha = \epsilon_p / \epsilon_f = 0$.
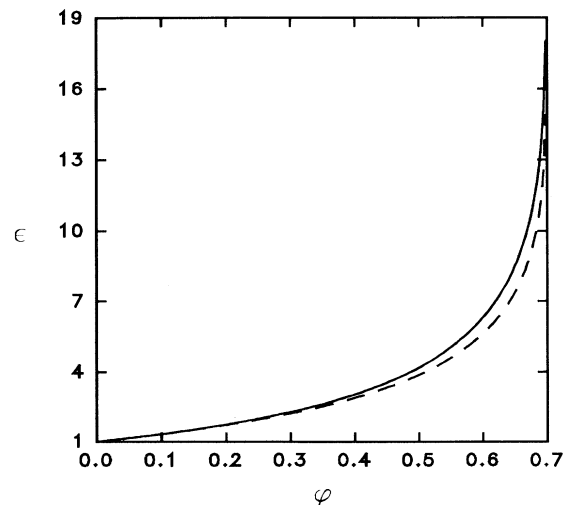

FIG. 3. The relative dielectric constants $\epsilon_{\parallel}$ (solid line) and $\epsilon_{\perp}$ (dashed line) as a function of the volume fraction φ for $\alpha = \epsilon_p / \epsilon_f = 100$.

TABLE IV. The dielectric constants of close packed configurations of the bct lattice (first two columns). Results for $\epsilon_\parallel$ and $\epsilon_{\rm fcc}$ obtained via the dipole approximation can be found in the last two columns.

α	$\epsilon_\parallel$	$\epsilon_\perp$	$\epsilon_\parallel^d$	$\epsilon_{\rm fcc}^d$
0	0.2249	0.1793	0.24	0.19
2	1.6513	1.6350	1.65	1.68
5	3.2428	3.0971	3.12	3.20
10	5.2542	4.8392	4.67	4.75
20	8.140	7.220	6.30	6.32
50	13.34	11.31	8.01	7.93
100	18.0	14.9	8.82	8.66

V. THE INDUCED DIPOLES
OF POLARIZABLE SPHERES ON A bct ARRAY

Recently some papers have appeared where the so-called electrostatic ground state of electrorheological fluids has been discussed [2,7,9]. In these papers it has generally been assumed that the electrostatic energy per particle should be minimum. The knowledge of the induced dipole moment of the particles in a periodic array is sufficient to determine the change in energy ΔW per particle [11],

$$\Delta W = -\tfrac{1}{2}\epsilon_f \mathbf{M}\cdot\mathbf{E} , \qquad (5.1)$$

with $\mathbf{M}$ the induced dipole moment of a particle in the array and $\mathbf{E}$ the averaged macroscopic electric field. The energy per particle can thus be minimized by maximizing the induced dipole on the particle. If the averaged macroscopic electric field is large the kinetic energy plays no significant role, consequently the most favorable structure is the one with the lowest electrostatic energy per particle [28]. Before we present the results we want to emphasize that an equivalent method is often used to determine the electrostatically most favorable structure [7]. If the relevant dielectric constant ratio $\tilde\epsilon = \epsilon/\epsilon_f$ is known it is also sufficient to study the quantity $(\tilde\epsilon - 1)/\varphi_{\rm CP}$, with $\varphi_{\rm CP}$ the close packed volume fraction.

First we consider the lowest-order solution of Eq. (3.19) for the calculation of the component $C_\parallel$ of the tensor $\underline{C}$ [see Eq. (4.1)]. We have then the following simple relation:

$$\beta_1 a^3 E_z = (1 - 2\beta_1 x^3 S_{20}^z)M_z = C_\parallel M_z . \qquad (5.2)$$

In this equation $x = a/R$, with R the distance of lattice sites along the x axis. Using $x^3 = 3\varphi/16\pi$ for the fcc lattice and $x^3 = \varphi\sqrt{6}/8\pi$ for the bct lattice we obtain $C_\parallel = 1 - \beta_1\varphi\chi_\parallel$, with $\chi_\parallel = 1$ for the fcc array and $\chi_\parallel = 1.0922364$ for the bct array. If we introduce the normalized volume fraction, $\tilde\varphi = \varphi/\varphi_{\rm CP}$ (with $\varphi_{\rm CP}^{\rm fcc} = \pi/3\sqrt{2}$ and $\varphi_{\rm CP}^{\rm bct} = 2\pi/9$), and use of $(\chi\varphi_{\rm CP})^{\rm fcc} = 0.7404804$, and $(\chi_\parallel\varphi_{\rm CP})^{\rm bct} = 0.7625248$, we see

$$\Delta = \frac{M_z^{\rm bct}}{M_z^{\rm fcc}} = \frac{(1 - 0.7405\beta_1\tilde\varphi)}{(1 - 0.7625\beta_1\tilde\varphi)} . \qquad (5.3)$$

The bct lattice is more stable than the fcc lattice if $\Delta > 1$, or if $\beta_1\tilde\varphi > 0$ (or $\alpha > 1$). This argumentation has been used by Tao and Sun to show that, in the dipolar approximation, the free energy per particle in the bct lattice is lower than in several other lattices [2]. For conducting spheres Davis has shown that $\Delta = 1$ by using an expansion in particle separation [7]. In Table V we show that the assumption of Tao and Sun is also valid if converged values of the induced dipoles of polarizable particles are calculated (including many higher-order multipole moments). These final values are denoted by Δ_∞. We have used the value of Davis for $\alpha = \infty$ because our method is not suitable to produce results in that particular case. The values for $\alpha = 10$ and 100, respectively, are accurate up to the last figure. From these results we may conclude that the free energy per particle remains lower for the bct lattice if $\alpha > 1$, but the differences from the fcc case are considerably more subtle. For $\alpha = 0$ we see that a reverse behavior is favored: the fcc structure is more stable than the bct one. Of course, this case is not interesting for ER fluids, but could be checked experimentally. It should be interesting to study surface effects in more detail for intermediate values of α, which are relevant for ER fluids, to gain more insight in how surface tension influences the free energy per particle in these systems. In this context we would like to emphasize that for slabs with a low number of layers a local simple cubic structure is sometimes more favorable than a local bcc structure [10]. This is related with an anomalous surface energy for the sc structure. Recently Toor and Halsey have presented some results of calculations of the surface energy for several lattice structures in the so-called constant dipole approximation [9]. They have also emphasized the anomalous behavior of the surface energy of the sc structure. It is important to consider this point more carefully for several lattice structures in relation with the electrostatic stability. Besides the surface effects another contribution to the free energy may play a role since the difference in free energy per particle for both close packed structures is less than 1% if $\alpha > 10$. We can think of temperature effects such as lattice vibrations.

Finally we want to briefly discuss some recently published results concerning a comparison of the electrostatic energy of close packed fcc and bct structures obtained by Friedberg and Yu [29]. They have studied the electrostatic energy of these lattices including the dipole, octupole, and 32-pole contribution in their calculations. The results of this approach are equivalent to those obtained by our method with $L = 5$ (see Sec. III A). However, we have performed calculations up to $L = 75$ which is neces-

TABLE V. The induced dipole moment of a particle in a bct array divided by the induced dipole moment of a particle in a fcc array. Δ: dipole approximation, Δ_∞: exact calculation.

α	Δ	Δ_∞
0	0.992	0.979
10	1.039	1.010
100	1.082	1.008
∞	1.093	1.000

sary when α is large. Nevertheless we may conclude that their results show the same trend that the difference in electrostatic energy per particle between the bct and fcc structure becomes much smaller if more multipoles are included. Friedberg and Yu have noted that for the bct structure the octupole moment is anomalously small. Our results confirm this point. We explain this by the large difference between the lattice sums S_{40} for the bct and fcc structures, respectively. From Table I we see that $S_{40}^{\text{bct}} = 0.0981$, but for the fcc case we have obtained $S_{40}^{\text{fcc}} = -7.5257$ (see also Ref. [14]).

VI. THE MANY-BODY ELECTROSTATIC FORCE AS FUNCTION OF THE MULTIPOLE MOMENTS

The electrostatic force between two spherical particles of equal size was studied by Davis [30] and Arp and Mason [31] for perfectly conducting spheres using bispherical coordinates. They obtained analytical expressions for the interparticle force, and lubricationlike expressions for two nearly touching spheres were presented by Arp and Mason. More recently Klingenberg has derived a method to calculate the interparticle force for the more general case of two polarizable particles. His method is numerical and restricted to the case of two spheres in an external electric field. The electrostatic force between two neighboring particles in an infinite chain has been studied by Chen, Sprecher, and Conrad [32]. The electrostatic interactions among all the spheres in the chain have been included. Their results indicate that the interparticle forces are approximately an order of magnitude higher than predicted by the point-dipole approximation. In this section we show that it is possible to derive an analytical expression for the interparticle force which is also valid for the determination of the electrostatic force among particles in the many-body problem contrarily to the results obtained using a bispherical coordinate system. Our many-particle result for the interparticle force is, of course, also valid for the two-particle case. Then we can compare our results for two-particle electrostatic forces to those obtained by Klingen-

berg [20] and, for perfectly conducting spheres, by Arp and Mason [31].

The knowledge of the electrostatic forces acting on the particles in an ER fluid is fundamental since their rheological behavior will depend on the balance between hydrodynamic and electrostatic forces. When the latter dominate, the solid particles agglomerate into aggregates elongated in the direction of the field. Because of the high concentration of the particles in these structures which are the building blocks of ER fluids, we have to take into account the many-body nature of the electrostatic interactions. Knowing the electrostatic and the hydrodynamic forces on each particle, their trajectory can then be obtained using Stokesian dynamics simulation [33]. This method has recently been used to simulate sheared electrorheological fluids [18,19,34]. In one of these papers, by Bonnecaze and Brady [19], a method to calculate numerically the electrostatic forces has been introduced which is similar to the one previously introduced to calculate hydrodynamic interactions [33]. The accuracy of such a method which mixes long-range many-body interactions with short-range interactions between pairs of spheres could now be tested against our analytical results.

In order to obtain an expression for the electrostatic force on particle i in the suspension, we have to determine the integral introduced in Sec. II [Eq. (2.9)],

$$\mathbf{F}_i = a^2 \int_{|\mathbf{r}_i|=a} \underline{T}(\mathbf{r}_i) \cdot \hat{\mathbf{e}}_r d\Omega_i$$

$$= \frac{\epsilon_f a^2}{4\pi} \int_{|\mathbf{r}_i|=a} \{ \mathbf{E}_{\text{out}}(\mathbf{r}_i) \mathbf{E}_{\text{out}}(\mathbf{r}_i)$$

$$- \tfrac{1}{2} \underline{I} [\mathbf{E}_{\text{out}}(\mathbf{r}_i) \cdot \mathbf{E}_{\text{out}}(\mathbf{r}_i)] \} \cdot \hat{\mathbf{e}}_r d\Omega_i \ ,$$

$$(6.1)$$

where we have assumed that we approach the particle surface from the fluid side. We have to determine an expression for the electric field in the fluid, defined with respect to the origin of particle i. Using $\mathbf{E}_{\text{out}} = -\nabla \varphi_{\text{out}}$, we obtain

$$\mathbf{E}_{\text{out}}(|\mathbf{r}_i|=a) = \mathbf{E}_0 - \sum_{\substack{l\,(\geq 1) \\ m}} \frac{4\pi}{2l+1} Q_{lm}^i a^{-(l+2)} \mathbf{B}_{lm}(\theta_i, \varphi_i)$$

$$- \sum_{\substack{s\,(\geq 1) \\ t}} a^{s-1} \mathbf{A}_{st}(\theta_i, \varphi_i) \left[\frac{n_{st}}{(s+t)!} \sum_{j\,(\neq i)} \sum_{\substack{l\,(\geq 1) \\ m}} \frac{4\pi}{2l+1} Q_{lm}^j M_{lm;st}^{ji}(\mathbf{R}_{ij}) \right] \ . \tag{6.2}$$

The functions $\mathbf{A}_{lm}(\theta, \varphi)$ and $\mathbf{B}_{lm}(\theta, \varphi)$ are vector spherical harmonics (see for references and discussion Ref. [22]). These vector functions have the following form:

$$\mathbf{A}_{lm}(\theta, \varphi) \equiv l Y_{lm}(\theta, \varphi) \hat{\mathbf{e}}_r + \frac{\partial Y_{lm}(\theta, \varphi)}{\partial \theta} \hat{\mathbf{e}}_\theta + \frac{1}{\sin\theta} \frac{\partial Y_{lm}(\theta, \varphi)}{\partial \varphi} \hat{\mathbf{e}}_\varphi \ , \tag{6.3}$$

$$\mathbf{B}_{lm}(\theta, \varphi) \equiv -(2l+1) Y_{lm}(\theta, \varphi) \hat{\mathbf{e}}_r + \mathbf{A}_{lm}(\theta, \varphi) \ , \tag{6.4}$$

with $\hat{\mathbf{e}}_r$, $\hat{\mathbf{e}}_\theta$, and $\hat{\mathbf{e}}_\varphi$ unit vectors in a spherical coordinate system. The last part of Eq. (6.2) can be eliminated with the help of Eq. (3.10), which also eliminates the explicit reference to the external field $\mathbf{E}_0$. The final result is

$$\mathbf{E}_{\text{out}}(|\mathbf{r}_i|=a)= \sum_{\substack{l\,(\geq 1)\\ m}} \frac{4\pi}{2l+1} Q^i_{lm} a^{-(l+2)} \left[\frac{1}{\beta_l} \mathbf{A}_{lm}(\theta_i,\varphi_i) - \mathbf{B}_{lm}(\theta_i,\varphi_i) \right]$$

$$\equiv 4\pi \sum_{\substack{l\,(\geq 1)\\ m}} Q^i_{lm} a^{-(l+2)} \frac{1}{l(\alpha-1)} \mathbf{X}_{lm}(\theta_i,\varphi_i) \ . \tag{6.5}$$

We do not consider the explicit form of the vector function $\mathbf{X}_{lm}(\theta,\varphi)$ in detail here. This is presented in the Appendix. Combination of this equation for the electric field in the fluid with the expression for the electrostatic force gives

$$\mathbf{F}_i = 4\pi\epsilon_f a^2 \sum_{\substack{l\,(\geq 1)\\ m}} \sum_{\substack{p\,(\geq 1)\\ q}} Q^i_{lm} Q^i_{pq} a^{-(l+p+4)} \frac{1}{lp(\alpha-1)^2} \int \left[\mathbf{X}_{lm} \mathbf{X}_{pq} - \frac{1}{2} \underline{I}\, [\mathbf{X}_{lm}\cdot\mathbf{X}_{pq}] \right] \cdot \hat{\mathbf{e}}_r d\Omega \ . \tag{6.6}$$

An outline of the calculation of the integral is presented in the Appendix. Substitution of the final result for the integral [Eq. (A8)] into the expression of $\mathbf{F}_i$, and using furthermore the generalized multipole moments [Eq. (3.14)] leads to the final expression for the force. The final calculus is straightforward and we do not present it. The Cartesian components of the force $\mathbf{F}_i$ are

$$F_{i,x} = -\tfrac{1}{4}\epsilon_f a^2 \sum_{\substack{l\,(\geq 1)\\ m}} (A^{+i}_{l,m} A^{+i}_{l+1,m+1} - A^{-i}_{l,m} A^{-i}_{l+1,m+1})$$

$$\times \frac{1}{\beta_{l+1}} \frac{(l+m+2)!}{(l-m)!} \ , \tag{6.7}$$

$$F_{i,y} = -\tfrac{1}{4}i\epsilon_f a^2 \sum_{\substack{l\,(\geq 1)\\ m}} (A^{+i}_{l,m} A^{-i}_{l+1,m+1} - A^{-i}_{l,m} A^{+i}_{l+1,m+1})$$

$$\times \frac{1}{\beta_{l+1}} \frac{(l+m+2)!}{(l-m)!} \ , \tag{6.8}$$

$$F_{i,z} = -\tfrac{1}{4}\epsilon_f a^2 \sum_{\substack{l\,(\geq 1)\\ m}} (A^{+i}_{l,m} A^{+i}_{l+1,m} - A^{-i}_{l,m} A^{-i}_{l+1,m})$$

$$\times \frac{1}{\beta_{l+1}} \frac{(l+m+1)!}{(l-m)!} \ . \tag{6.9}$$

We emphasize that these results are valid for an arbitrary number of particles interacting electrostatically. The many-body interactions, i.e., the geometry of N-particle cluster, are implicitly accounted for in the values of the generalized multipole moments. It is obvious that our expressions for the components of $\mathbf{F}_i$ are easy to evaluate numerically.

VII. THE TWO-PARTICLE ELECTROSTATIC FORCE: A COMPARISON

In this section we compare our theoretical expression for the electrostatic force to analytical results of Arp and Mason [31] for the force between two perfectly conducting spheres and numerical data of Klingenberg [20] for the force between two polarizable spheres in an externally applied electric field. In order to do this comparison we have to relate our force expression to the one used by Klingenberg. Suppose we place particle 1 at the origin of a Cartesian coordinate system while the other lies on the

negative z axis at a distance R. The externally applied electric field is in the xz plane and has an angle θ with the z axis. The force on the particle 2 is then [20]

$$\mathbf{F}_2 = 3\epsilon_f a^2 \beta_1^2 E_0^2 x^4 [(2f_{2,\|}\cos^2\theta - f_{2,\perp}\sin^2\theta)\hat{\mathbf{e}}_z$$

$$- f_{2,\Gamma}\sin 2\theta\,\hat{\mathbf{e}}_x] \ , \tag{7.1}$$

with $\beta=(\alpha-1)/(\alpha+2)$ and $x=a/R$. In this equation we have a minus sign instead of a plus sign in front of the coefficient $f_{2,\Gamma}$. This is due to the configuration of our two-particle pair in the externally applied electric field. It is not difficult to show that all generalized multipole moments A^{-i}_{lm} are zero (thus $F_{i,y}=0$). We may then identify the following relations:

$$f_{2,\|} = -\frac{1}{6x^4(A^{+2}_{10})^2} \sum_{l\,(\geq 1)} \frac{l+1}{\beta_{l+1}} A^{+2}_{l,0} A^{+2}_{l+1,0} \ , \tag{7.2}$$

$$f_{2,\perp} = \frac{1}{6x^4(A^{+2}_{11})^2} \sum_{l\,(\geq 1)} \frac{l(l+1)(l+2)}{\beta_{l+1}} A^{+2}_{l,1} A^{+2}_{l+1,1} \ , \tag{7.3}$$

$$f_{2,\Gamma} = -\frac{1}{12x^4 A^{+2}_{10} A^{+2}_{11}}$$

$$\times \sum_{l\,(\geq 1)} \frac{1}{\beta_{l+1}} [l(l+1)A^{+2}_{l,1} A^{+2}_{l+1,0}$$

$$-(l+1)(l+2)A^{+2}_{l,0} A^{+2}_{l+1,1}] \ . \tag{7.4}$$

To demonstrate the correctness of our method we have calculated values of the force functions $f_\|, f_\perp$, and f_Γ for the most difficult case of conducting spheres ($\alpha=\infty$) and compared them to the exact results of Arp and Mason. For this comparison we have expressed the values obtained by Arp and Mason in terms of the force functions used in this paper. We may conclude from the examination of Table VI that the multipole expansion results are in good agreement with those of Arp and Mason. The small differences can be explained by the fact that the data of Arp and Mason have a four-digit accuracy only, with, of course, an uncertainty in the last digit of their results. That our expression leads to good results can be seen if we consider the force function $f_\perp$ for touching spheres. It is not difficult to obtain results consistent with the analytical expression obtained by Arp and

TABLE VI. The force coefficients $f_\parallel$, $f_\perp$, and f_Γ are compared with those obtained by Arp and Mason [31] for perfectly conducting spheres ($\alpha = \infty$). The latter are denoted by the subscript AM.

R/a	$f_\parallel$	$f_{AM,\parallel}$	$f_\perp$	$f_{AM,\perp}$	f_Γ	$f_{AM,\Gamma}$
2.0000		∞	0.555 721 3	0.555 721 3	(3.1)	4.006 856
2.0002	587.23	587.4	0.555 84	0.556 4	2.7032	2.706
2.0006	239.74	239.8	0.556 08	0.555 9	2.5619	2.562
2.0020	91.548	91.57	0.556 90	0.556 9	2.3712	2.371
2.0060	38.645	38.65	0.559 26	0.559 2	2.1573	2.157
2.0200	15.231	15.23	0.567 46	0.567 8	1.8763	1.876
2.0600	6.6126	6.612	0.590 53	0.590 5	1.5901	1.590

Mason using an expansion in ξ with $\xi = (R/a - 2) \ll 1$. This expression is (Table 2, Ref. [31]) $f_{AM,\perp} = 2\zeta(3) - \frac{8}{3}\ln 2$, with $\zeta(3) = 1.202\,056\,9$. From the same table of Arp and Mason we can determine the values of the other force functions in the case of touching spheres. $f_{AM,\parallel}$ diverges and $f_{AM,\Gamma} = 10\zeta(3)/3$. Our result for f_Γ has still not been converged to its final value; this is the only case where the multipole expansion does not lead to a satisfactory result.

In Table VII we present some values obtained for the three force functions defined in Eq. (7.1) for $\alpha = 10$ and 100, and for different normalized separations between the spheres. All the data are converged up to the last digit. We have compared some of them with the few available data in this range of interparticle separations calculated by Klingenberg [20]. The Klingenberg results (with 0.01% accuracy) are very well reproduced. However, we want to point out that with the analytic expression of the electrostatic force we are able to calculate these functions for high values of α when the particles are in contact. Recently Klingenberg et al. have presented extrapolation formulas to calculate the force functions for all interparticle separations because they could not obtain these values with their numerical method to determine these functions [18]. Their approximate functions have for each α a set of fitting parameters which are tabulated in Ref. [18] for $\alpha \in \{2, 4, 10, \infty\}$. With these approximate functions we obtain for $\alpha = 10$ the following results for the force functions: $f_\parallel = 7.293$, $f_\perp = 0.618$, and $f_\Gamma = 1.496$. This is in agreement with our data within

their error margins. Also Bonnecaze and Brady have presented some results for the force functions for the touching sphere configuration [19]. Their approach was to calculate the electrostatic forces from the derivative of the electrostatic energy, which is also an exact approach. For $\alpha = 10$ they have calculated $f_\parallel = 5.17$, $f_\perp = 0.63$, and $f_\Gamma = 1.44$. The difference with the exact results, especially for $f_\parallel$, is large. We do not know the reason for this discrepancy. In their paper they have compared these results with extrapolated values of the force functions obtained by using graphical data which were presented by Gast and Zukoski [17,35]. These extrapolated values are $f_\parallel = 5.20$, $f_\perp = 0.62$, $f_\Gamma = 1.46$. These results are in reasonable agreement with those of Bonnecaze and Brady, but unfortunately these data are not very accurate, except the value for $f_\perp$. They have not presented results for higher values of α.

We conclude with the remark that our analytical expression for the electrostatic force seems to be the only one which gives correct results for the force functions in the entire interparticle range, and for all values of $\alpha = \epsilon_p / \epsilon_f$, with not too much computational effort. The method of Klingenberg suffices to calculate the force functions for all interparticle separations if $\alpha \sim 1$. They had to introduce approximation techniques to calculate the force functions in the entire interparticle range if $\alpha \geq 10$. The results of Arp and Mason are valid for conducting spheres ($\alpha = \infty$) only. We cannot judge about the method of Bonnecaze and Brady, more data are necessary in that case.

TABLE VII. The coefficients $f_\parallel$, $f_\perp$, and f_Γ for $\alpha = 10$ and 100. Some of them are compared with those obtained by Klingenberg [20] for polarizable spheres (denoted by KL).

α	R/a	$f_\parallel$	$f_{KL,\parallel}$	$f_\perp$	$f_{KL,\perp}$	f_Γ	$f_{KL,\Gamma}$
10	2.0000	7.2870		0.6192		1.5035	
	2.0020	6.8441		0.6204		1.4933	
	2.0060	6.2021		0.6227		1.4749	
	2.0200	4.9332		0.6307		1.4244	
	2.0600	3.4708	3.472	0.6529	0.6529	1.3328	1.3328
	2.1000	2.8275	2.8279	0.6743	0.6743	1.2753	1.2753
100	2.0000	182.21		0.5624		2.3087	
	2.0020	51.802		0.5636		2.1509	
	2.0060	27.883		0.5659		2.0153	
	2.0200	12.881		0.5741		1.7988	
	2.0600	6.0721	6.075	0.5972	0.5972	1.5520	1.5520
	2.1000	4.2731	4.2739	0.6195	0.6195	1.4321	1.4321

VIII. THREE-PARTICLE CONTRIBUTIONS TO THE ELECTROSTATIC FORCE

We shall now present the results of a study of the electrostatic force acting on the particles in a three-particle cluster. We consider two special configurations which are suitable to show the importance of incorporating three-particle contributions in the study of, e.g., the restoring force used in theories to describe yield stress phenomena in ER or magnetorheological (MR) fluids. The first configuration under consideration is one where we have situated all particles on a line. Particle 1 has been put in the origin of a coordinate system, and particles 2 and 3 on the negative z axis. In the second configuration, we have put the three particles on the corners of an equilateral triangle. This configuration has the advantage that the particles can touch each other simultaneously. We have chosen these two configurations because the first one is of interest in the study of the restoring force on particles aligned with a specified angle with respect to an externally applied electric field. The other one may be of interest because these configurations appear in dense structures.

We consider now the first configuration. We can use the set of linear equations introduced in Sec. III B. The particles are situated on the z axis with

$$|\mathbf{R}_{12}|=|\mathbf{R}_{23}|\equiv R, \quad |\mathbf{R}_{13}|=2R ,$$

$$\xi_{12}=0, \quad \xi_{13}=0, \quad \xi_{23}=0 . \tag{8.1}$$

Substitution of Eq. (8.1) into our set of linear equations [Eqs. (3.15) and (3.16)] for the respective interparticle distances and angles leads to a considerably simplified set of linear equations. The set of liner equations is decoupled concerning the azimuthal indices, and the functions $P_{lm;pq}^{\pm ji}$ are real functions (the phase factors in the spherical harmonics are equal to unity). The latter has the advantage that we can solve the set of algebraic equations independently for the coefficients A_{lm}^{+j} and A_{lm}^{-j}. These simplifications make it possible to study solutions of the set of linear equations with taking into account many multipole moments. The largest value of the upper limit used in one of our calculations was $L=500$. Using the symmetry of the particle configuration it is sufficient to assume that the externally applied electric field is in the xz plane (the angle between the z axis and the applied field vector is denoted by θ). Consequently we have to deal with the solution of the coefficients A_{lm}^{+j}, with $j\in\{1,2,3\}$, in terms of the external field only.

It is often assumed that the electrostatic force acting on a particle in a cluster of polarizable spheres can be described using the assumption of additivity of the two-particle forces. If we apply this assumption for the calculation of the force on particle 1 we obtain, using the notation introduced by Klingenberg [20],

$$\mathbf{F}_1=-3\epsilon_f a^2\beta_1^2 E_0^2 x^4[(2F_{\|}\cos^2\theta-F_{\perp}\sin\theta)\hat{\mathbf{e}}_z$$

$$-F_{\Gamma}(\sin2\theta)\hat{\mathbf{e}}_x] , \tag{8.2}$$

with $x=a/R$ and θ the angle between the z axis and the externally applied electric field. The modified Klingenberg force functions are now

$$F_{2\kappa}=f(R)_\kappa+\tfrac{1}{16}f(2R)_\kappa, \quad \kappa\in\{\|,\perp,\Gamma\} . \tag{8.3}$$

This relation can be obtained by considering the sum of the electrostatic force on particle 1 caused by the other two particles taking into account that $x_{13}=a/R_{13}=\tfrac{1}{2}x$. We have calculated the exact three-particle values of the force functions $(F_{3\kappa})$ and tabulated the results normalized by the force functions $F_{2\kappa}$, for four values of $\alpha=\epsilon_p/\epsilon_f$ ($\infty,100,10,0$) in Table VIII. The calculations are performed for $R\in\{2,2.01,2.1,2.5,4\}$. It is remarkable that the three-particle contribution to the electrostatic force is so large. The three-particle contribution to the electrostatic force is for nearly touching spheres of the same order as the two-particle contribution. We see that even for relatively large interparticle distances the three-particle contribution is substantial. We might expect that even fourth and higher-order contributions are significant. In Figs. 4–6 we have plotted the normalized values of the functions $F_{3\|}$, $F_{3\perp}$, and $F_{3\Gamma}$ for $\alpha=10$ and 100 as a function of L, the number of multipole moments used in the calculation. We can conclude that especially the lower-order multipole moments contribute to the final result, although we see for higher values of α that we need many multipole moments to obtain a reasonably converged value. Furthermore we see from Figs. 4–6 that including induced dipoles and quadrupoles in the calculation of the force functions ($L=2$) is not sufficient to obtain qualitatively correct results. It is difficult to obtain converged values for the normalized force functions

TABLE VIII. The three-particle force functions $F_{3\kappa}$, with $\kappa\in\{\|,\perp,\Gamma\}$ normalized by the modified two-particle force functions, with $F_{2\kappa}=f_\kappa(R)+\tfrac{1}{16}f_\kappa(2R)$ [see Eq. (8.3)].

α	R/a	$F_{3\|}/F_{2\|}$	$F_{3\perp}/F_{2\perp}$	$F_{3\Gamma}/F_{2\Gamma}$
∞	2.000	1.9	0.914	1.39
	2.010	1.534	0.915	1.235
	2.100	1.329	0.924	1.131
	2.500	1.149	0.950	1.049
	4.000	1.034	0.985	1.009
100	2.000	1.584	0.916	1.263
	2.010	1.476	0.917	1.209
	2.100	1.310	0.926	1.123
	2.500	1.144	0.952	1.047
	4.000	1.033	0.985	1.009
10	2.000	1.255	0.934	1.109
	2.010	1.247	0.935	1.103
	2.100	1.197	0.942	1.075
	2.500	1.103	0.962	1.033
	4.000	1.025	0.988	1.007
0	2.000	0.914	1.045	0.988
	2.010	0.915	1.045	0.988
	2.100	0.924	1.041	0.987
	2.500	0.950	1.026	0.989
	4.000	0.985	1.008	0.996

FIG. 4. The normalized force function $F_{3\parallel}/F_{2\parallel}$ as a function of the number of multipole moments L used in its calculation. The upper curve represents results for $\alpha=100$ and the lower one for $\alpha=10$.
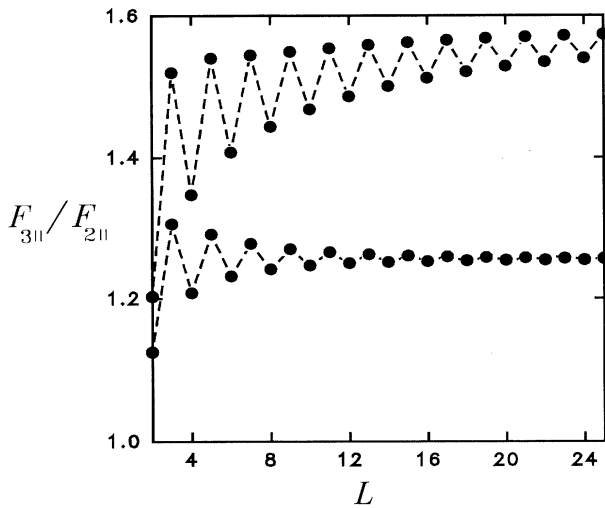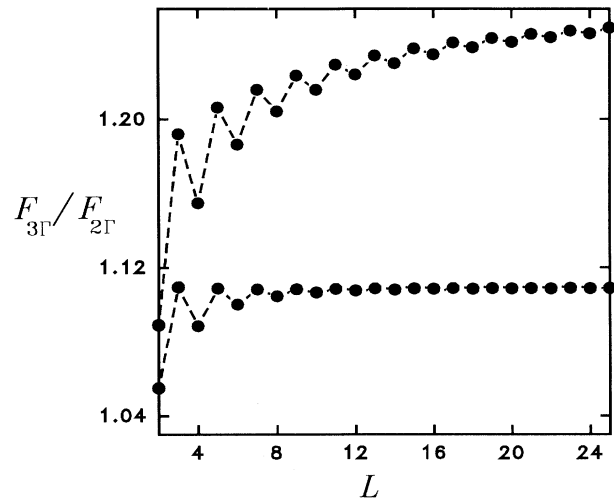

FIG. 6. The normalized force function $F_{3\Gamma}/F_{2\Gamma}$ as a function of the number of multipole moments L used in its calculation. The upper curve represents results for $\alpha=100$ and the lower one for $\alpha=10$.

$F_{3\parallel}$ and $F_{3\Gamma}$ for the case of touching conducting spheres. The presented values should be taken with care because convergence behavior could be very slow. The calculations are performed by taking into account up to 500 multipole moments ($L=500$) and the limiting results, especially for $F_{3\parallel}$, may be considered as a lower bound. In Fig. 7 we have plotted the normalized force function $F_{3\parallel}/F_{2\parallel}$ as a function of the multipole moments. From this figure, and the behavior of the functions for touching spheres in the case of increasing α, and the behavior of the force functions for conducting spheres in the case of decreasing interparticle distance, we may conclude that $[F_{3\kappa}/F_{2\kappa}]_{\alpha=\infty,R/a=2}\neq 1$ ($\kappa\in\{\parallel,\perp,\Gamma\}$). This means that the lubrication forces between two nearly touching particles are strongly influenced by the third particle. The

values of the electrostatic force on the other two particles are trivial. The electrostatic force on particle 2 is zero, and the one on particle 3 is related to the force on particle 1, $\mathbf{F}_3=-\mathbf{F}_1$.

In the study of the static yield stress of sheared ER or MR fluids it is generally assumed that the electrostatic forces are pairwise additive. This means in practice nearest-neighbor interactions only. Klingenberg and Zukoski have derived a theoretical expression for the static yield stress based on the assumptions mentioned above [36]. They have modeled the ER suspension as a two-dimensional array of chains of particles spanning the electrodes. The chains are sheared and on each particle a restoring force is exerted. This restoring force has the following form [36]:
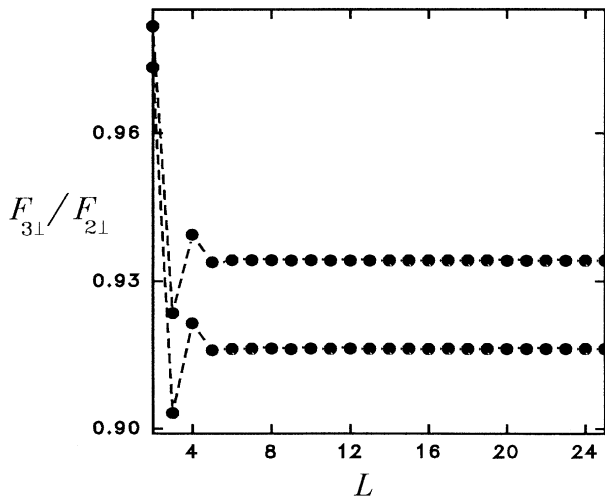

FIG. 5. The normalized force function $F_{3\perp}/F_{2\perp}$ as a function of the number of multipole moments L used in its calculation. The upper curve represents results for $\alpha=10$ and the lower one for $\alpha=100$.
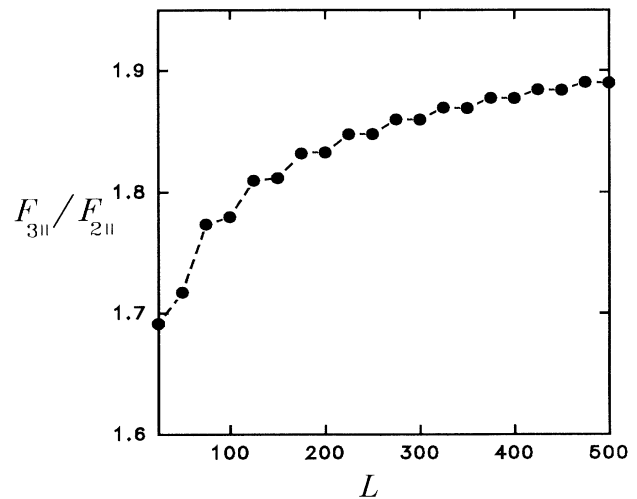

FIG. 7. The normalized force function $F_{3\parallel}/F_{2\parallel}$ for touching conducting spheres as a function of the number of multipole moments used in the calculation.

$$F_{\text{res}} = 3\epsilon_f a^2 \beta_1^2 E_0^2 x^4 [(2F_\parallel + 2F_\Gamma) \sin\theta \cos^2\theta - F_\perp \sin^3\theta] \, ,$$

$$(8.4)$$

where θ is the angle with which the chains are tilted (the electric field is perpendicular to the electrodes). The configuration for three particles is shown in Fig. 8. Klingenberg et al. assumed that at some critical value of the strain, which is assumed to be related to the maximum restoring force, the chains will break and will reform with the nearest-neighbor chain. They have derived an expression for the static yield stress which is among others a linear function of the maximum value of the dimensionless restoring force F_m and a function of the angle θ_m at which the restoring force is maximum. They have calculated the values F_m and θ_m for several values of $\alpha \leq 15$. We have calculated these values for several values of α, including three-particle contributions, and tabulated them in Table IX. We have compared the values with those obtained using two-particle interactions only. The main conclusion is that the values of the maximum restoring force are roughly between 20% and 50% higher than calculated with the additivity assumption of the electrostatic forces. The values of θ_m are slightly lower (2–10%) than the previously calculated values. Recently experimental results have been reported concerning the static yield stress in MR fluids [37]. The measured yield stress values were roughly 40% lower than the theoretically obtained values based on the pair additivity assumption. If we include three-particle interactions the discrepancy even grows to about 100%.

The second configuration is more complicated. We have put particle 1 in the origin of a Cartesian coordinate system, particle 2 on the negative z axis, and the third particle in the xz plane (Fig. 9). The interparticle distances are all equal, $|\mathbf{R}_{12}| = |\mathbf{R}_{13}| = |\mathbf{R}_{23}| = R$. Furthermore $\xi_{12} = 0$, $\xi_{13} = \frac{1}{3}\pi$, and $\xi_{23} = \frac{2}{3}\pi$. In the present case we cannot simplify the set of linear algebraic equations by using a decoupling procedure concerning the azimuthal indices. This has major consequences for the choice of the upper limit L. In the problem described above we had to solve $3L$ linear equations, but in the case of three particles on the corners of an equilateral triangle we have to solve $3L(L+2)$ linear equations. The only simplification is again the decoupling of the set of equations concerning the general multipole moments A_{lm}^{+j} and A_{lm}^{-j}. From this decoupling we may conclude that the y
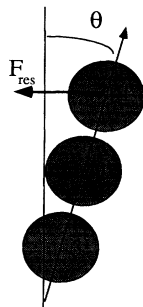
TABLE IX. A comparison of the two- and three-particle restoring forces, $F_{m,2}$ and $F_{m,3}$, respectively, together with the values $\theta_{m,2}$ and $\theta_{m,3}$ at which these forces are maximum.

α	$F_{m,2}$	$F_{m,3}$	$\theta_{m,2}$	$\theta_{m,3}$
5	0.0927	0.1064	17.11	16.83
10	0.1200	0.1454	13.91	13.37
15	0.1396	0.1756	11.77	11.08
20	0.1554	0.2011	10.17	9.42
25	0.1688	0.2236	8.91	8.14
50	0.2206	0.3150	5.16	4.60
100	0.2996	0.4598	2.51	2.29

component of the electrostatic force is zero if the applied electric field is in the xz plane or equivalently, no force component in the xz plane is the applied field is parallel to the y axis. There exists, of course, another formulation of the problem where one may use explicitly the fact that the three-particle cluster has a threefold rotation axis. However, computer programs are available to solve the set of linear equations for the configuration with the particles in the xz plane. This program is convenient for our purpose so we do not expound this particular approach. In Table X we have presented results for the force exerted on particle 3 in the case of an external field parallel to the z axis and x axis, respectively. The tabulated data are normalized by the pure two-particle electrostatic force which can be obtained by using the following two expressions:

$$F_{3x} = -\tfrac{3}{4}\sqrt{3}\epsilon_f a^2 \beta_1^2 E_0^2 x^4 (2f_\parallel + 2f_\Gamma - 3f_\perp) \, ,$$

$$\text{with } \mathbf{E}_0 \| \hat{\mathbf{e}}_z \, ,$$

$$(8.5)$$

$$F_{3x} = -\tfrac{3}{4}\sqrt{3}\epsilon_f a^2 \beta_1^2 E_0^2 x^4 (6f_\parallel - 2f_\Gamma - f_\perp) \, ,$$

$$\text{with } \mathbf{E}_0 \| \hat{\mathbf{e}}_x \, .$$

We have to consider the x component of the electrostatic force only, because the z component is always zero by symmetry arguments. Although the separate two-particle forces in the x direction are attractive (i.e., directed to the center of the triangle) we may conclude that the attractive force in the three-particle cluster is much less than the sum of the two-particle contributions. The two-particle approach leads in this case to a strong overestimation of the attractive electrostatic forces in contrast to the first configuration discussed in this section where the particles are stuck together more strongly than calculated in the two-particle approach. It is interesting to note that these remarks remain valid for intermediate particle separations, and also for low values of α.

FIG. 8. Illustration of the tilted three-particle configuration used to calculate the restoring force on particle 1.
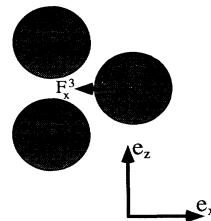

FIG. 9. The three-particle triangle configuration with the x component of the electrostatic force on particle 3.

TABLE X. The three-particle electrostatic force exerted on particle 3 (F_3), normalized by the force obtained by using the assumption of additivity of two-particle forces, for several values of α and interparticle separations. In the second column: $\mathbf{E}_0 \| \hat{\mathbf{e}}_z$, in the last column: $\mathbf{E}_0 \| \hat{\mathbf{e}}_x$.

α	R/a	F_3/F_2 (E_z)	F_3/F_2 (E_x)
100	2.00	0.56	0.56
	2.05	0.634	0.621
	2.10	0.664	0.637
	2.20	0.706	0.651
	2.50	0.790	0.686
25	2.00	0.615	0.611
	2.05	0.656	0.636
	2.10	0.681	0.646
	2.20	0.719	0.658
	2.50	0.800	0.696
10	2.00	0.671	0.653
	2.05	0.691	0.657
	2.10	0.711	0.662
	2.20	0.744	0.672
	2.50	0.820	0.714
2	2.00	0.835	0.755
	2.05	0.846	0.760
	2.10	0.856	0.767
	2.20	0.876	0.784
	2.50	0.920	0.839

Finally we want to emphasize the following point. The normalized force functions converge more quickly to their final values than the explicit results for the two- and three-particle electrostatic forces, respectively. However, reliable results for the two-particle electrostatic forces (or the so-called Klingenberg force functions) up to touching sphere configurations are easily obtained by our method for $\alpha \leq 100$. This is related to a decoupling procedure concerning the azimuthal indices discussed above. The effect of fast convergence behavior of the normalized forces to a value not equal to one seems to indicate that the lubricationlike forces for nearly touching spheres in the three-sphere cluster is not simply a sum of the two-particle lubrication forces. This can also be shown by considering the pure three-particle contribution to the electrostatic force. This contribution has the same convergence behavior as the two-particle contribution.

We can conclude this section by remarking that it is not sufficient to consider two-particle electrostatic interactions only if studying the forces among polarizable particles. The three-particle contributions are of the same order as the two-particle contributions and the final effect on the behavior of three-particle clusters is not trivial. Furthermore it has been shown that a simple approach by considering the lowest-order multipoles only (induced dipoles and quadrupoles) does not give very accurate results for the force functions for higher values of α (see Figs. 4–7). The remark made by Klingenberg, Van Swol, and Zukoski that the multibody contributions to the pair electrostatic interactions are insensitive to the details of the structure seems incorrect [18].

IX. CONCLUSION

In this paper we have presented a method to study many-particle electrostatic interactions using the theory of multipole expansions. We have been able to reformulate the obtained set of linear algebraic equations in a way suitable to perform calculations for both periodic arrays as the N-particle cluster with arbitrary particle configurations. The results obtained with this method for the dielectric constants of cubic arrays, and for the force functions of Klingenberg to describe two-particle electrostatic forces, are in perfect agreement with results from the literature.

We have presented rigorous calculations, including higher-order multipole moments, for the dielectric constants of the bct array, and the induced dipole moments of the particles in that array. First we may conclude that the claim of Tao and Sun which states that the bct structure should be more favorable than the fcc or hcp structure is justified, although they used a dipolar approach only. However, the differences with the fcc structure are much smaller than those calculated by Tao and Sun (for $\alpha = 100$, typical for ER fluids, a factor 10 lower). Consequently we may expect that surface and temperature effects play a more important role than previously assumed. Its precise role should be investigated in more detail. Another conclusion is that the diagonal components of the dielectric tensor of the bct array at close packed configurations are always lower than the dielectric constant of the fcc array at close packed configurations for $1 < \alpha < \infty$ contrarily to the results obtained with the dipolar approach if $\alpha \geq 25$. We have considered in this comparison only close packed configurations, but we may expect that it is also valid for more dilute arrays.

Using the theory of multipole expansion we have obtained an analytical expression for the many-particle electrostatic forces in terms of generalized multipole moments. This expression is simple as is its numerical implementation. We want to emphasize the fact that we did not make any special assumptions concerning the geometry of the N-particle cluster under consideration. This expression is used to study three-particle contributions to the electrostatic force and the conclusion is that these contributions can be as important as the two-particle contribution if the interparticle separation is not too large. In particular, for three aligned conducting spheres which are almost touching, the rate of divergence of the force between two particles is almost two times the rate of divergence for two spheres alone. Our many-body expression may be used in various studies of the behavior of electrorheological fluids, e.g., in a theory describing rupture effects in ER fluids or in dynamic simulation methods.

APPENDIX

We present an outline of the calculation of the following integral:

$$\int \{\mathbf{X}_{lm}(\theta,\varphi)\mathbf{X}_{pq}(\theta,\varphi)-\tfrac{1}{2}\underline{I}[\mathbf{X}_{lm}(\theta,\varphi)\cdot\mathbf{X}_{pq}(\theta,\varphi)]\}\cdot\hat{\mathbf{e}}_r d\Omega \;,$$

(A1)

with $\mathbf{X}_{lm}(\theta,\varphi)$ a shorthand notation for

$$\mathbf{X}_{lm}(\theta,\varphi)\equiv\alpha l Y_{lm}(\theta,\varphi)\hat{\mathbf{e}}_r+\frac{\partial Y_{lm}(\theta,\varphi)}{\partial\theta}\hat{\mathbf{e}}_\theta+\frac{1}{\sin\theta}\frac{\partial Y_{lm}(\theta,\varphi)}{\partial\varphi}\hat{\mathbf{e}}_\varphi \;,$$

(A2)

with $\hat{\mathbf{e}}_r$, $\hat{\mathbf{e}}_\theta$, and $\hat{\mathbf{e}}_\varphi$ the unit vectors in a spherical coordinate system and α some arbitrary constant. The integrand of Eq. (A1) can be written in the following way:

$$\left[\mathbf{X}_{lm}\mathbf{X}_{pq}-\frac{1}{2}\underline{I}(\mathbf{X}_{lm}\cdot\mathbf{X}_{pq})\right]\cdot\hat{\mathbf{e}}_r=\frac{1}{2}\alpha^2 lp Y_{lm}(Y_{pq}\hat{\mathbf{e}}_r)-\frac{1}{2}\frac{\partial Y_{lm}}{\partial\theta}\frac{\partial(Y_{pq}\hat{\mathbf{e}}_r)}{\partial\theta}-\frac{1}{2\sin^2\theta}\frac{\partial Y_{lm}}{\partial\varphi}\frac{\partial(Y_{pq}\hat{\mathbf{e}}_r)}{\partial\varphi}$$

$$+\frac{1}{2}(2\alpha p+1)\left[\frac{\partial Y_{lm}}{\partial\theta}Y_{pq}\hat{\mathbf{e}}_\theta+\frac{1}{\sin\theta}\frac{\partial Y_{lm}}{\partial\varphi}Y_{pq}\hat{\mathbf{e}}_\varphi\right] \;.$$

(A3)

We may express $Y_{pq}\hat{\mathbf{e}}_r$, which is in fact a product of spherical harmonics, in terms of single spherical harmonics by using the following expressions:

$$n_{11}Y_{1,1}Y_{pq}=\left[\frac{(p+q+1)(p+q+2)}{(2p+1)(2p+3)}\right]^{1/2}Y_{p+1,q+1}$$
$$-\left[\frac{(p-q)(p-q-1)}{(2p+1)(2p-1)}\right]^{1/2}Y_{p-1,q+1} \;,$$

$$n_{11}Y_{1,-1}Y_{pq}=\left[\frac{(p-q+1)(p-q+2)}{(2p+1)(2p+3)}\right]^{1/2}Y_{p+1,q-1}$$
$$-\left[\frac{(p+q)(p+q-1)}{(2p+1)(2p-1)}\right]^{1/2}Y_{p-1,q-1} \;,$$

$$n_{10}Y_{1,0}Y_{pq}=\left[\frac{(p+q+1)(p-q+1)}{(2p+1)(2p+3)}\right]^{1/2}Y_{p+1,q}$$
$$+\left[\frac{(p+q)(p-q)}{(2p+1)(2p-1)}\right]^{1/2}Y_{p-1,q} \;.$$

Furthermore we may identify the following relation:

$$\frac{\partial Y_{lm}}{\partial\theta}\frac{\partial Y_{st}}{\partial\theta}+\frac{1}{\sin^2\theta}\frac{\partial Y_{lm}}{\partial\varphi}\frac{\partial Y_{st}}{\partial\varphi}=\mathbf{C}_{lm}\cdot\mathbf{C}_{st} \;,$$

(A4)

with $\mathbf{C}_{lm}$ vector spherical harmonics as introduced in Ref. [22]. The first part of Eq. (A1) can be determined using the following relations:

$$\int Y_{lm}(\theta,\varphi)Y_{st}(\theta,\varphi)d\Omega=(-1)^m\delta_{l,s}\delta_{-m,t} \;,$$

(A5)

$$\int \mathbf{C}_{lm}(\theta,\varphi)\cdot\mathbf{C}_{st}(\theta,\varphi)d\Omega=(-1)^m l(l+1)\delta_{l,s}\delta_{-m,t} \;.$$

(A6)

The remaining part of Eq. (A3) (the last term between large parentheses) is more difficult to evaluate. We introduce first the following differential operators (see, e.g., Messiah [38]):

$$L_\pm Y_{lm}=e^{\pm i\varphi}\left[\pm\frac{\partial Y_{lm}}{\partial\theta}+i\cot\theta\frac{\partial Y_{lm}}{\partial\varphi}\right] \;.$$

(A7)

With these operators we are able to express the relation

$$\frac{\partial Y_{lm}}{\partial\theta}\hat{\mathbf{e}}_\theta+\frac{1}{\sin\theta}\frac{\partial Y_{lm}}{\partial\varphi}\hat{\mathbf{e}}_\varphi$$

in terms of single spherical harmonics. The orthonormality relation (A5) is then sufficient to determine also the final part of integral (A1). The complete calculation of this integral is straightforward, and we restrict ourselves to the presentation of the final result only, which has the following form:

$$\int\left[\mathbf{X}_{lm}(\theta,\varphi)\mathbf{X}_{pq}(\theta,\varphi)-\frac{1}{2}\underline{I}[\mathbf{X}_{lm}(\theta,\varphi)\cdot\mathbf{X}_{pq}(\theta,\varphi)]\right]\cdot\hat{\mathbf{e}}_r d\Omega$$

$$=\frac{1}{2}(-1)^m l[(l+1)\alpha^2-2\alpha(l+1)-(l+2)]\left[\frac{1}{2}(\hat{\mathbf{e}}_x-i\hat{\mathbf{e}}_y)\left[\frac{(l+m+1)(l+m+2)}{(2l+1)(2l+3)}\right]^{1/2}\delta_{q,-m-1}\right.$$

$$-\frac{1}{2}(\hat{\mathbf{e}}_x+i\hat{\mathbf{e}}_y)\left[\frac{(l-m+1(l-m+2)}{(2l+1)(2l+3)}\right]^{1/2}\delta_{q,-m+1}$$

$$\left.+\hat{\mathbf{e}}_z\left[\frac{(l+m+1)(l-m+1)}{(2l+1)(2l+3)}\right]^{1/2}\delta_{q,-m}\right]\delta_{p,l+1}$$

$$+\frac{1}{2}(-1)^m(l-1)[l\alpha^2+2\alpha(l+1)-(l+1)]\left[-\frac{1}{2}(\hat{\mathbf{e}}_x-i\hat{\mathbf{e}}_y)\left[\frac{(l-m)(l-m-1)}{(2l+1)(2l-1)}\right]^{1/2}\delta_{q,-m-1}\right.$$

$$+\frac{1}{2}(\hat{\mathbf{e}}_x+i\hat{\mathbf{e}}_y)\left[\frac{(l+m)(l+m-1)}{(2l+1)(2l-1)}\right]^{1/2}\delta_{q,-m+1}$$

$$\left.+\hat{\mathbf{e}}_z\left[\frac{(l+m)(l-m)}{(2l+1)(2l-1)}\right]^{1/2}\delta_{q,-m}\right]\delta_{p,l-1} \;.$$

(A8)

*Present address: Department of Physics, Eindhoven University of Technology, P.O. Box 513, 5600 MB Eindhoven, The Netherlands.

[1] T. C. Halsey, Science **258**, 761 (1992).

[2] R. Tao and J. M. Sun, Phys Rev. Lett. **67**, 398 (1991).

[3] T. Chen, R. N. Zitter, and R. Tao, Phys. Rev. Lett. **68**, 2555 (1992).

[4] T. C. Halsey and W. Toor, Phys. Rev. Lett. **65**, 2820 (1990).

[5] Y. Grasselli, G. Bossis, and E. Lemaire (unpublished).

[6] R. Tao and J. M. Sun, Phys. Rev. A **44**, 6181 (1991).

[7] L. C. Davis, Phys. Rev. A **46**, 719 (1992).

[8] G. K. Batchelor and R. W. O'Brien, Proc. R. Soc. London Ser. A **355**, 313 (1977).

[9] W. R. Toor and T. C. Halsey, Phys. Rev. A **45**, 8617 (1992).

[10] H. J. H. Clercx and G. Bossis, J. Chem. Phys. **98**, 8284 (1993).

[11] J. D. Jackson, *Classical Electrodynamics,* 2nd ed. (Wiley, New York, 1975), Chaps. 4 and 6.

[12] M. Sancho, G. Martinez, and M. Llamas, J. Electrostatics **21**, 135 (1988).

[13] R. C. McPhedran and D. R. McKenzie, Proc. R. Soc. London Ser. A **359**, 45 (1978).

[14] A. S. Sangani and A. Acrivos, Proc. R. Soc. London Ser. A **386**, 263 (1983).

[15] J. Lam, J. Appl. Phys. **60**, 4230 (1986).

[16] R. D. Miller and T. B. Jones, J. Phys. D **21**, 527 (1988).

[17] A. P. Gast and C. F. Zukoski, Adv. Colloid Interface Sci. **30**, 153 (1989).

[18] D. J. Klingenberg, F. van Swol, and C. F. Zukoski, J. Chem. Phys. **94**, 6170 (1991).

[19] R. T. Bonnecaze and J. F. Brady, J. Chem. Phys. **96**, 2183 (1992).

[20] D. J. Klingenberg, Ph.D. thesis, University of Illinois, 1990.

[21] R. T. Bonnecaze and J. F. Brady, Proc. R. Soc. London Ser. A **430**, 285 (1990).

[22] H. J. H. Clercx and P. P. J. M. Schram, Physica A **174**, 293 (1991).

[23] H. J. H. Clercx and P. P. J. M. Schram, J. Chem. Phys. **96**, 3137 (1992).

[24] B. R. A. Nijboer and F. W. de Wette, Physica **23**, 309 (1957).

[25] J. W. S. Rayleigh, Philos. Mag. **34**, 481 (1892).

[26] D. R. McKenzie, R. C. McPhedran, and G. H. Derrick, Proc. R. Soc. London Ser. A **362**, 211 (1978).

[27] W. T. Doyle, J. Appl. Phys. **49**, 795 (1978).

[28] R. Tao, J. T. Woestman, and N. K. Jaggi, Appl. Phys. Lett. **55**, 1844 (1989).

[29] R. Friedberg and Y. Yu, Phys. Rev. B **46**, 6582 (1992).

[30] M. H. Davis, Q. J. Mech. Appl. Math. **17**, 499 (1964).

[31] P. A. Arp and S. G. Mason, Colloid Polym. Sci. **255**, 566 (1977).

[32] Y. Chen, A. F. Sprecher, and H. Conrad, J. Appl. Phys. **70**, 6796 (1991).

[33] J. F. Brady and G. Bossis, Annu. Rev. Fluid Mech. **20**, 111 (1988).

[34] D. J. Klingenberg, F. van Swol, and C. F. Zukoski, J. Chem. Phys. **94**, 6160 (1991).

[35] R. T. Bonnecaze and J. F. Brady, in *Proceedings of the Second International Conference on ER Fluids,* edited by J. D. Carlson, A. F. Sprecher, and H. Conrad (Technomic, Lancaster, PA, 1990).

[36] D. J. Klingenberg and C. F. Zukoski, Langmuir **6**, 15 (1990).

[37] E. Lemaire and G. Bossis, J. Phys. D **24**, 1473 (1991).

[38] A. Messiah, *Quantum Mechanics I* (North-Holland, Amsterdam, 1981), pp. 492–496.